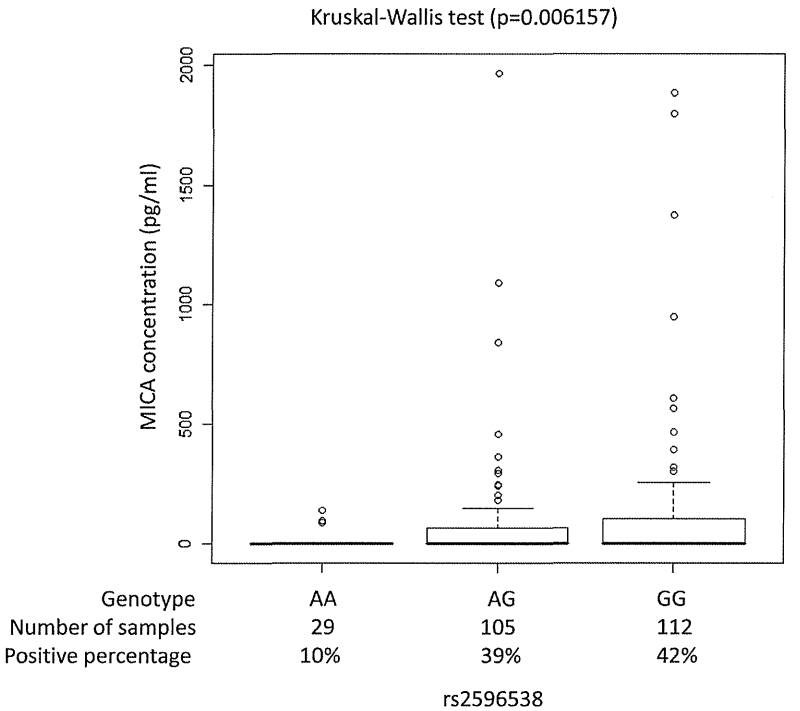

Figure 4. Association between the soluble MICA levels and SNP rs2596538 genotype. The samples were classified into 3 groups according to rs2596538 genotype. The sMICA levels measured by ELISA are indicated in y-axis. The numbers of samples and the proportion of sMICA positive subjects from each group are shown in x-axis. The percentage of the positive sMICA expression in each group are AA = 10%, AG = 39%, and GG = 42%. Statistical significance was determined by Kruskal-Wallis test.
doi:10.1371/journal.pone.0061279.g004

ubiquitously expressed transcription factor which binds to the GC-rich decanucleotide sequence (GC box) and activates the transcription of various viral and cellular genes [30,31]. Phosphorylation of SP1 was shown to be induced by HCV core protein and exhibited higher binding affinity to the promoter region of its downstream targets [32]. From our previous study, we showed a significant difference of sMICA expression between non-HCV individuals and CHC patients. This indicated that sMICA expression was induced after HCV infection [6]. Hence, we here propose the following hypothesis. After HCV infection, the virus core protein enhances the SP1 phosphorylation in hepatocytes, and the phosphorylated SP1 binds to the DNA segment corresponding to the G allele of SNP rs2596538 and then induces *MICA* expression. The membrane-bound MICA (mMICA) serves as a ligand for NKG2D to activate the immune system and results in the elimination of viral-infected cells by NK cells and CD8+ T cells [8,9]. Eventually, HCV-infected individuals with higher MICA level may cause stronger immune response to the infected cells and hence result in a reduced risk for HCC progression. Moreover, the mMICA is then shed by metalloproteinases that are often over-expressed in cancer tissues and convert mMICA to sMICA. This resulted in a significantly increase of sMICA level in the serum of HCV infected patients.

In contrast to HCV-induced HCC, our group had previously identified that higher sMICA level was associated with poor prognosis in HBV-induced HCC patients [33]. Such an opposite effect of *MICA* would be attributable to the difference in downstream pathway between HBV and HCV. HBV virus encodes hepatitis B virus X protein (HBx) that is pathogenic and promotes tumor formation. It had been reported that HBx protein was associated with an elevated expression of MT1-MMP, MMP2, and MMP3 [34,35]. HBx was also shown to transactivate MMP9 through ERKs and PI-3K-AKT/PKB pathway and suppress TIMP1 and TIMP3 activities [36,37]. The activation of metalloproteinases would induce the shedding of mMICA into sMICA, which promotes the tumor formation through the inhibitory effect of sMICA on NK cells. This can explain why high sMICA expression is a marker of poor prognosis for HBV-induced HCC. On the other hand, HCV infection was not associated with metalloproteinases activation, although the expression of sMICA was shown to be proportional to mMICA level. Therefore individuals with high MICA expression are likely to activate natural killer cells and CD8+ T cells to eliminate virus infected cells.

SP1 was previously identified as a transcriptional regulator of both *MICA* and *MICB* [7,9,38]. A polymorphism in the *MICB* promoter region was found to be associated with *MICB* transcription level [7]. To our knowledge, this is the first report showing that *MICA* transcription is directly influenced by functional variant. Moreover, this functional SNP is significantly associated with HCV-induced HCC. Our findings provide an insight that *MICA* genetic variation is a promising prognostic biomarker for CHC patients.

Supporting Information

Figure S1 Pairwise LD map between marker SNP and 11 candidates SNP. Black color boxes represent regions of high pairwise r^2 value. The LD was determined by direct DNA

sequencing of *MICA* promoter region from 50 randomly selected HCV-HCC patients.
(TIF)

Table S1 Characteristics of samples and methods used in this study.
(DOCX)

Table S2 The sequences of each oligo used in the EMSA and ChIP assay.
(DOCX)

Table S3 Copy number variation between HCV-HCC and control samples.
(DOCX)

Author Contributions

Conceived and designed the experiments: PHYL YN KM. Performed the experiments: PHYL YU VK. Analyzed the data: PHYL YU CT. Contributed reagents/materials/analysis tools: KK NK DM KC MK. Wrote the paper: PHYL KM.

References

1. Umemura T, Ichijo T, Yoshizawa K, Tanaka E, Kiyosawa K (2009) Epidemiology of hepatocellular carcinoma in Japan. J Gastroenterol 44 Suppl 19: 102–107.
2. Fassio E (2010) Hepatitis C and hepatocellular carcinoma. Ann Hepatol 9 Suppl: 119–122.
3. Mbarek H, Ochi H, Urabe Y, Kumar V, Kubo M, et al. (2011) A genome-wide association study of chronic hepatitis B identified novel risk locus in a Japanese population. Hum Mol Genet 20: 3884–3892.
4. Kamatani Y, Wattanapokayakit S, Ochi H, Kawaguchi T, Takahashi A, et al. (2009) A genome-wide association study identifies variants in the HLA-DP locus associated with chronic hepatitis B in Asians. Nat Genet 41: 591–595.
5. Zhang H, Zhai Y, Hu Z, Wu C, Qian J, et al. (2010) Genome-wide association study identifies 1p36.22 as a new susceptibility locus for hepatocellular carcinoma in chronic hepatitis B virus carriers. Nat Genet 42: 755–758.
6. Kumar V, Kato N, Urabe Y, Takahashi A, Muroyama R, et al. (2011) Genome-wide association study identifies a susceptibility locus for HCV-induced hepatocellular carcinoma. Nat Genet 43: 455–458.
7. Rodríguez-Rodero S, González S, Rodrigo L, Fernández-Morera JL, Martínez-Borra J, et al. (2007) Transcriptional regulation of MICA and MICB: a novel polymorphism in MICB promoter alters transcriptional regulation by Sp1. Eur J Immunol 37: 1938–1953.
8. Bauer S, Groh V, Wu J, Steinle A, Phillips JH, et al. (1999) Activation of NK cells and T cells by NKG2D, a receptor for stress-inducible MICA. Science 285: 727–729.
9. Zhang C, Wang Y, Zhou Z, Zhang J, Tian Z (2009) Sodium butyrate upregulates expression of NKG2D ligand MICA/B in HeLa and HepG2 cell lines and increases their susceptibility to NK lysis. Cancer Immunol Immunother 58: 1275–1285.
10. Sun D, Wang X, Zhang H, Deng L, Zhang Y (2011) MMP9 mediates MICA shedding in human osteosarcomas. Cell Biol Int 35: 569–574.
11. Waldhauer I, Goehlsdorf D, Gieseke F, Weinschenk T, Wittenbrink M, et al. (2008) Tumor-associated MICA is shed by ADAM proteases. Cancer Res 68: 6368–6376.
12. Jinushi M, Takehara T, Tatsumi T, Kanto T, Groh V, et al. (2003) Expression and role of MICA and MICB in human hepatocellular carcinomas and their regulation by retinoic acid. Int J Cancer 104: 354–361.
13. Kohga K, Takehara T, Tatsumi T, Ohkawa K, Miyagi T, et al. (2008) Serum levels of soluble major histocompatibility complex (MHC) class I-related chain A in patients with chronic liver diseases and changes during transcatheter arterial embolization for hepatocellular carcinoma. Cancer Sci 99: 1643–1649.
14. Ota M, Katsuyama Y, Mizuki N, Ando H, Furihata K, et al. (1997) Trinucleotide repeat polymorphism within exon 5 of the MICA gene (MHC class I chain-related gene A): allele frequency data in the nine population groups Japanese, Northern Han, Hui, Uygur, Kazakhstan, Iranian, Saudi Arabian, Greek and Italian. Tissue Antigens 49: 448–454.
15. Nakamura Y (2007) The BioBank Japan Project. Clin Adv Hematol Oncol 5: 696–697.
16. Tanikawa C, Urabe Y, Matsuo K, Kubo M, Takahashi A, et al. (2012) A genome-wide association study identifies two susceptibility loci for duodenal ulcer in the Japanese population. Nat Genet 44: 430–434, S431–432.
17. Miki D, Ochi H, Hayes CN, Abe H, Yoshima T, et al. (2011) Variation in the DEPDC5 locus is associated with progression to hepatocellular carcinoma in chronic hepatitis C virus carriers. Nat Genet 43: 797–800.
18. Urabe Y, Ochi H, Kato N, Kumar V, Takahashi A, et al. (2013) A genome-wide association study of HCV induced liver cirrhosis in the Japanese population identifies novel susceptibility loci at MHC region. J Hepatol.
19. Scott LJ, Mohlke KL, Bonnycastle LL, Willer CJ, Li Y, et al. (2007) A genome-wide association study of type 2 diabetes in Finns detects multiple susceptibility variants. Science 316: 1341–1345.
20. Consortium GP (2010) A map of human genome variation from population-scale sequencing. Nature 467: 1061–1073.
21. Venkataraman GM, Suciu D, Groh V, Boss JM, Spies T (2007) Promoter region architecture and transcriptional regulation of the genes for the MHC class I-related chain A and B ligands of NKG2D. J Immunol 178: 961–969.
22. Andrews NC, Faller DV (1991) A rapid micropreparation technique for extraction of DNA-binding proteins from limiting numbers of mammalian cells. Nucleic Acids Res 19: 2499.
23. Hata J, Matsuda K, Ninomiya T, Yonemoto K, Matsushita T, et al. (2007) Functional SNP in an Sp1-binding site of AGTRL1 gene is associated with susceptibility to brain infarction. Hum Mol Genet 16: 630–639.
24. Barrett JC (2009) Haploview: Visualization and analysis of SNP genotype data. Cold Spring Harb Protoc 2009: pdb.ip71.
25. Komatsu-Wakui M, Tokunaga K, Ishikawa Y, Leelayuwat C, Kashiwase K, et al. (2001) Wide distribution of the MICA-MICB null haplotype in East Asians. Tissue Antigens 57: 1–8.
26. Tse KP, Su WH, Yang ML, Cheng HY, Tsang NM, et al. (2011) A gender-specific association of CNV at 6p21.3 with NPC susceptibility. Hum Mol Genet 20: 2889–2896.
27. Negro F, Alberti A (2011) The global health burden of hepatitis C virus infection. Liver Int 31 Suppl 2: 1–3.
28. Cabibbo G, Craxi A (2010) Epidemiology, risk factors and surveillance of hepatocellular carcinoma. Eur Rev Med Pharmacol Sci 14: 352–355.
29. McGlynn KA, London WT (2011) The global epidemiology of hepatocellular carcinoma: present and future. Clin Liver Dis 15: 223–243.
30. Kadonaga JT, Tjian R (1986) Affinity purification of sequence-specific DNA binding proteins. Proc Natl Acad Sci U S A 83: 5889–5893.
31. Suske G (1999) The Sp-family of transcription factors. Gene 238: 291–300.
32. Lee S, Park U, Lee YI (2001) Hepatitis C virus core protein transactivates insulin-like growth factor II gene transcription through acting concurrently on Egr1 and Sp1 sites. Virology 283: 167–177.
33. Kumar V, Yi Lo PH, Sawai H, Kato N, Takahashi A, et al. (2012) Soluble MICA and a MICA Variation as Possible Prognostic Biomarkers for HBV-Induced Hepatocellular Carcinoma. PLoS One 7: e44743.
34. Ou DP, Tao YM, Tang FQ, Yang LY (2007) The hepatitis B virus X protein promotes hepatocellular carcinoma metastasis by upregulation of matrix metalloproteinases. Int J Cancer 120: 1208–1214.
35. Yu FL, Liu HJ, Lee JW, Liao MH, Shih WL (2005) Hepatitis B virus X protein promotes cell migration by inducing matrix metalloproteinase-3. J Hepatol 42: 520–527.
36. Chung TW, Lee YC, Kim CH (2004) Hepatitis B viral HBx induces matrix metalloproteinase-9 gene expression through activation of ERK and PI-3K/AKT pathways: involvement of invasive potential. FASEB J 18: 1123–1125.
37. Kim JR, Kim CH (2004) Association of a high activity of matrix metalloproteinase-9 to low levels of tissue inhibitors of metalloproteinase-1 and -3 in human hepatitis B-viral hepatoma cells. Int J Biochem Cell Biol 36: 2293–2306.
38. Andresen L, Jensen H, Pedersen MT, Hansen KA, Skov S (2007) Molecular regulation of MHC class I chain-related protein A expression after HDAC-inhibitor treatment of Jurkat T cells. J Immunol 179: 8235–8242.

Research Article

EASL EUROPEAN ASSOCIATION FOR THE STUDY OF THE LIVER | JOURNAL OF HEPATOLOGY

The transcription factor SALL4 regulates stemness of EpCAM-positive hepatocellular carcinoma

Sha Sha Zeng[1], Taro Yamashita[1,2,*], Mitsumasa Kondo[1], Kouki Nio[1], Takehiro Hayashi[1], Yasumasa Hara[1], Yoshimoto Nomura[1], Mariko Yoshida[1], Tomoyuki Hayashi[1], Naoki Oishi[1], Hiroko Ikeda[3], Masao Honda[1], Shuichi Kaneko[1]

[1]*Department of Gastroenterology, Kanazawa University Hospital, Kanazawa, Ishikawa, Japan;* [2]*Department of General Medicine, Kanazawa University Hospital, Kanazawa, Ishikawa, Japan;* [3]*Department of Pathology, Kanazawa University Hospital, Kanazawa, Ishikawa, Japan*

Background & Aims: Recent evidence suggests that hepatocellular carcinoma can be classified into certain molecular subtypes with distinct prognoses based on the stem/maturational status of the tumor. We investigated the transcription program deregulated in hepatocellular carcinomas with stem cell features.

Methods: Gene and protein expression profiles were obtained from 238 (analyzed by microarray), 144 (analyzed by immunohistochemistry), and 61 (analyzed by qRT-PCR) hepatocellular carcinoma cases. Activation/suppression of an identified transcription factor was used to evaluate its role in cell lines. The relationship of the transcription factor and prognosis was statistically examined.

Results: The transcription factor SALL4, known to regulate stemness in embryonic and hematopoietic stem cells, was found to be activated in a hepatocellular carcinoma subtype with stem cell features. SALL4-positive hepatocellular carcinoma patients were associated with high values of serum alpha fetoprotein, high frequency of hepatitis B virus infection, and poor prognosis after surgery compared with SALL4-negative patients. Activation of SALL4 enhanced spheroid formation and invasion capacities, key characteristics of cancer stem cells, and up-regulated the hepatic stem cell markers *KRT19*, *EPCAM*, and *CD44* in cell lines. Knockdown of SALL4 resulted in the down-regulation of these stem cell markers, together with attenuation of the invasion capacity. The SALL4 expression status was associated with histone deacetylase activity in cell lines, and the histone deacetylase inhibitor successfully suppressed proliferation of SALL4-positive hepatocellular carcinoma cells.

Conclusions: SALL4 is a valuable biomarker and therapeutic target for the diagnosis and treatment of hepatocellular carcinoma with stem cell features.

Keywords: Cancer stem cell; Hepatocellular carcinoma; Gene expression profile; Chemosensitivity.

Received 15 March 2013; received in revised form 27 August 2013; accepted 28 August 2013; available online 6 September 2013

* Corresponding author. Address: Department of General Medicine/Gastroenterology, Kanazawa University Hospital, 13-1 Takara-Machi, Kanazawa, Ishikawa 920-8641, Japan. Tel.: +81 76 265 2042; fax: +81 76 234 4281.

E-mail address: taroy@m-kanazawa.jp (T. Yamashita).

Abbreviations: CSC, cancer stem cell; HCC, hepatocellular carcinoma; EpCAM, epithelial cell adhesion molecule; AFP, alpha fetoprotein; HpSC-HCC, hepatic stem cell-like HCC; MH-HCC, mature hepatocyte-like HCC; SALL4, Sal-like 4 (Drosophila); qRT-PCR, quantitative reverse transcription-polymerase chain reaction; HDAC, histone deacetylase; SAHA, suberoylanilide hydroxamic acid; SBHA, suberic bis-hydroxamic acid; NuRD, nucleosome remodeling and deacetylase.

Introduction

Cancer is a heterogeneous disease in terms of morphology and clinical behavior. This heterogeneity has traditionally been explained by the clonal evolution of cancer cells and the accumulation of serial stochastic genetic/epigenetic changes [1]. The alteration of the microenvironment by tumor stromal cells is also considered to contribute to the development of the heterogeneous nature of the tumor through the activation of various signaling pathways in cancer cells, including epithelial mesenchymal transition programs [2].

Recent evidence suggests that a subset of tumor cells with stem cell features, known as cancer stem cells (CSCs), are capable of self-renewal and can give rise to relatively differentiated cells, thereby forming heterogeneous tumor cell populations [3]. CSCs were also found to generate tumors more efficiently in immunodeficient mice than non-cancer stem cells in various solid tumors as well as hematological malignancies [4]. CSCs are also more metastatic and chemo/radiation-resistant than non-CSCs and are therefore considered to be a pivotal target for tumor eradication [5,6].

Hepatocellular carcinoma (HCC) is a leading cause of cancer death worldwide [7]. Recently, we proposed a novel HCC classification system based on the expression status of the hepatic stem/progenitor markers epithelial cell adhesion molecule (EpCAM) and alpha fetoprotein (AFP) [8]. EpCAM-positive ($^+$) AFP$^+$ HCC (hepatic stem cell-like HCC; HpSC-HCC) is characterized by an onset of disease at younger ages, activation of Wnt/β-catenin signaling, a high frequency of portal vein invasion and poor

prognosis after radical resection, compared with EpCAM$^-$ AFP$^-$ HCC (mature hepatocyte-like HCC; MH-HCC) [9]. *EPCAM* is a target gene of Wnt/β-catenin signaling, and EpCAM$^+$ HCC cells isolated from primary HCC and cell lines show CSC features including tumorigenicity, invasiveness, and resistance to fluorouracil [9,10]. Thus, EpCAM appears to be a potentially useful marker for the isolation of liver CSCs in HpSC-HCC. However, key transcriptional programs responsible for the maintenance of EpCAM$^+$ CSCs are still unclear.

In this study, we aimed to clarify the transcriptional programs deregulated in HpSC-HCC using a gene expression profiling approach. We found that the *SALL4* gene encoding Sal-like 4 (*Drosophila*) (SALL4), a zinc finger transcriptional activator and vertebrate orthologue of the *Drosophila* gene spalt (*sal*) [11], was up-regulated in HpSC-HCC. In adults, *SALL4* is known to be expressed in hematopoietic stem cells and their malignancies, but its role in HCC has not yet been fully elucidated [12–14]. We therefore investigated the role of SALL4 in the regulation and maintenance of EpCAM$^+$ HCC.

Materials and methods

Clinical HCC specimens

A total of 144 HCC tissues and adjacent non-cancerous liver tissues were obtained from patients who underwent hepatectomy for HCC treatment from 2002 to 2010 at Kanazawa University Hospital, Kanazawa, Japan. These samples were formalin-fixed and paraffin-embedded, and used for immunohistochemistry (IHC). A further 61 HCC samples were obtained from patients who underwent hepatectomy from 2008 to 2011; these were freshly snap-frozen in liquid nitrogen and used for RNA analysis. Of these 61 HCCs, 8 and 36 cases were defined as HpSC-HCC and MH-HCC, respectively, according to previously described criteria [8].

27 HCC cases were included in both the IHC cohort (n = 144) and quantitative reverse transcription-polymerase chain reaction (qRT-PCR) cohort ($n = 61$), and SALL4 gene and protein expression were compared between these cases. An additional fresh HpSC-HCC sample was obtained from a surgically resected specimen and immediately used for preparation of a single-cell suspension. All experimental and tissue acquisition procedures were approved by the Ethics Committee and the Institutional Review Board of Kanazawa University Hospital. All patients provided written informed consent.

Microarray analysis

Detailed information on microarray analysis is available in the Supplementary Materials and methods.

Cell culture and reagents

Human liver cancer cell lines HuH1, HuH7, HLE, and HLF were obtained from the Japanese Collection of Research Bioresources (JCRB), and Hep3B and SK-Hep-1 were obtained from the American Type Culture Collection (ATCC). Single-cell suspensions of primary HCC tissue were prepared as described previously [15]. Detailed information is available in the Supplementary Materials and methods. The histone deacetylase (HDAC) inhibitor suberic bis-hydroxamic acid (SBHA) and suberoylanilide hydroxamic acid (SAHA) were obtained from Cayman Chemical (Ann Arbor, MI). Plasmid constructs pCMV6-SALL4 (encoding *SALL4A*), pCMV6-SALL4-GFP, and 29mer shRNA constructs against human SALL4 (No. 7412) were obtained from OriGene Technologies, Inc. (Rockville, MD). These constructs were transfected using Lipofectamine 2000 (Life Technologies, Carlsbad, CA) according to the manufacturer's protocol.

Western blotting

Whole cell lysates were prepared using RIPA lysis buffer. Nuclear and cytoplasmic proteins were extracted using NE-PER Nuclear and Cytoplasmic Extraction Reagents (Pierce Biotechnology Inc., Rockford, IL). Mouse monoclonal antibody to human Sall4 clone 6E3 (Abnova, Walnut, CA), rabbit polyclonal antibodies to human Lamin B1 (Cell Signaling Technology Inc., Danvers, MA), and mouse monoclonal anti-β-actin antibody (Sigma-Aldrich, St. Louis, MO) were used. Immune complexes were visualized by enhanced chemiluminescence (Amersham Biosciences Corp., Piscataway, NJ) as described previously [15,16].

Quantitative reverse transcription-polymerase chain reaction (qRT-PCR)

Detailed information on qRT-PCR is available in the Supplementary Materials and methods.

IHC and immunofluorescence (IF) analyses

IHC was performed using an Envision+ kit (Dako, Carpinteria, CA) according to the manufacturer's instructions. Anti-SALL4 monoclonal antibody 6E3 (Abnova, Walnut, CA), anti-EpCAM monoclonal antibody VU-1D9 (Oncogene Research Products, San Diego, CA), and anti-CK19 monoclonal antibody RCK108 (Dako Japan, Tokyo, Japan) were used for detecting SALL4, EpCAM, and CK19, respectively. Anti-Sall4 rabbit polyclonal antibodies (ab29112) (Abnova) and vector red (Vector Laboratories Inc., Burlingame, CA) were used for double color IHC analysis. Samples with >5% positive staining in a given area were considered to be positive for a particular antibody. For IF analyses, Alexa 488 fluorescein isothiocyanate (FITC)-conjugated anti-mouse immunoglobulin G (IgG) (Life Technologies) was used as a secondary antibody.

Cell proliferation, spheroid formation, invasion, and HDAC activity assay

Detailed information on this topic is available in the Supplementary Materials and methods.

Statistical analyses

Student's t tests were performed with GraphPad Prism software 5.0 (GraphPad Software, San Diego, CA) to compare various test groups assayed by cell proliferation assays and qRT-PCR analysis. Spearman's correlation analysis and Kaplan-Meier survival analysis were also performed with GraphPad Prism software 5.0 (GraphPad Software).

Results

Activation of SALL4 in HpSC-HCC

To elucidate the transcriptional programs deregulated in HpSC-HCC, we performed class-comparison analyses and identified 793 genes showing significant differences in differential expression between HpSC-HCC (n = 60) and MH-HCC (n = 96) ($p < 0.001$), as previously described [9]. Of them, 455 genes were specifically up-regulated in HpSC-HCC, and we performed transcription factor analysis using this gene set to identify their transcriptional regulators by MetaCore software. We identified four transcription factor genes, *SALL4*, *NFYA*, *TP53*, and *SP1*, that were potentially activated in HpSC-HCC (Fig. 1A). Involvement of *TP53* and *SP1* in the stemness of HCC has previously been described [17,18], but the roles of *SALL4* and *NFYA* were unclear.

We investigated the interaction networks affected by *SALL4* and *NFYA* using the MetaCore dataset. We showed that *SALL4* might be a regulator of Akt signaling (*SP1*), Wnt signaling (*TCF7L2*), and epigenetic modification (*JARID2*, *DMRT1*, *DNMT3B*) [19], and could potentially regulate two other transcriptional regulators, *SP1* and *NFYA*, through Akt and Myb signaling pathways (Fig. 1B). As a recent study indicated that *SALL4* is a direct target of the Wnt signaling pathway [20], which is dominantly activated in HpSC-HCC [9], we focused on the expression of *SALL4* in HpSC-HCC, and confirmed its up-regulation in HpSC-HCC compared

A

Transcription factors	*p* value	z-score
SALL4	0.0005708	3.958
NFYA	0.002483	3.267
TP53	3.923E-05	4.25
SP1	2.917E-11	6.942

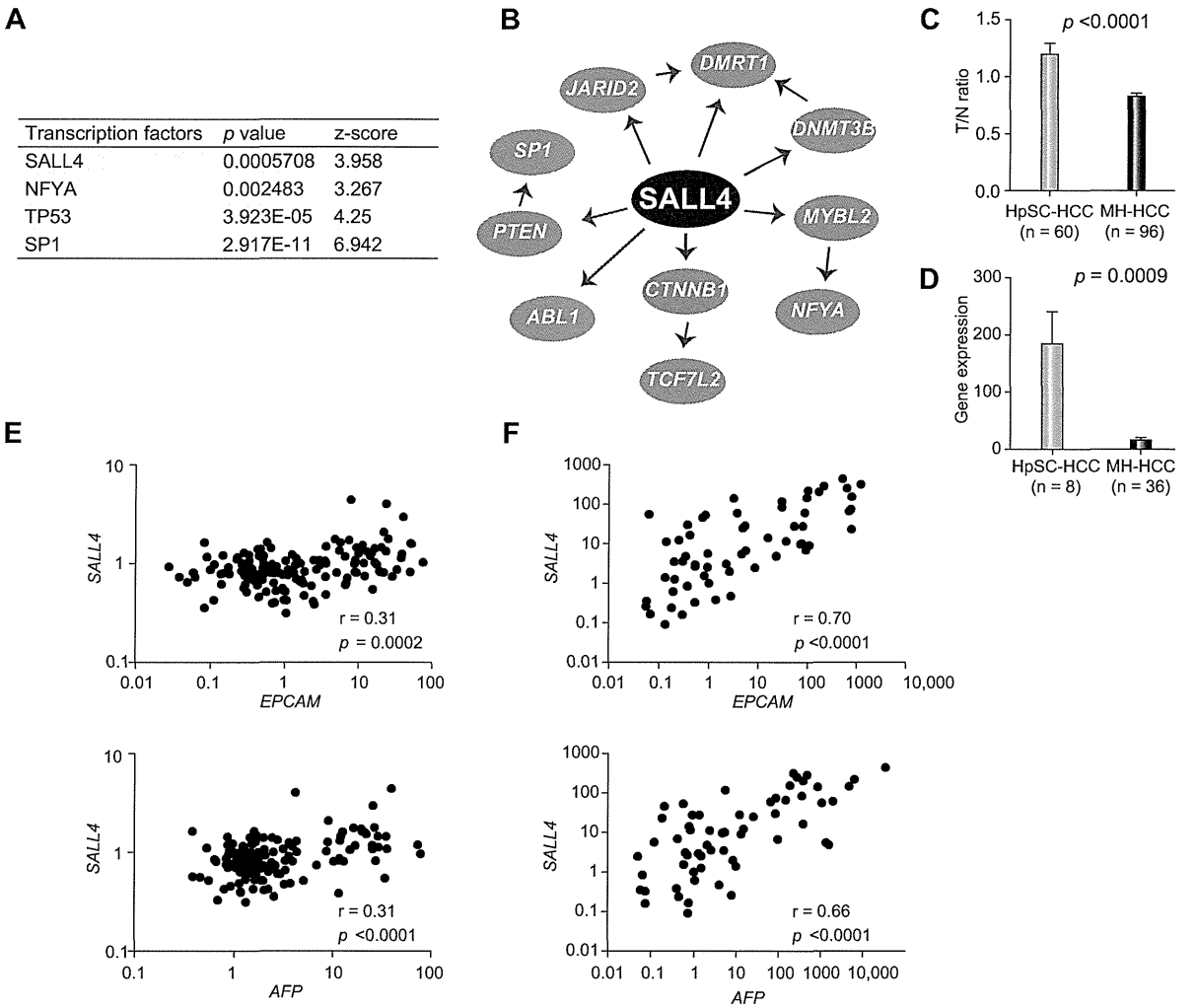

Fig. 1. Transcription factors potentially activated in HpSC-HCC. (A) Transcription factor analysis. Transcription factors regulating genes up-regulated in HpSC-HCC are listed with their *p* values and z-scores as calculated by MetaCore software. (B) Interaction network analysis. Seven genes (*ABL1*, *DMRT1*, *DNMT3B*, *JARID2*, *NFYA*, *SP1*, and *TCF7L2*, indicated in orange) shown to be up-regulated in HpSC-HCC were identified as potential target genes regulated by *SALL4* (indicated in red). (C) *SALL4* gene expression evaluated by microarray analysis. Tumor/non-tumor (T/N) ratios of microarray data in HpSC-HCC (n = 60) and MH-HCC (n = 96). (D) *SALL4* gene expression evaluated by qRT-PCR. Gene expression of *SALL4* in HpSC-HCC (n = 8) and MH-HCC (n = 36) samples. (E) Scatter plot analysis. Gene expression levels of *EPCAM* (upper panel) and *AFP* (lower panel) were positively correlated with those of *SALL4* in microarray data (n = 238, T/N ratios), as shown by Spearman's correlation coefficients. (F) Scatter plot analysis. Gene expression levels of *EPCAM* (upper panel) and *AFP* (lower panel) were positively correlated with those of *SALL4* in qRT-PCR data (n = 61), as shown by Spearman's correlation coefficients. (This figure appears in colour on the web.)

with MH-HCC as evaluated by microarray data (Fig. 1C). We validated this using an independent HCC cohort evaluated by qRT-PCR (Fig. 1D). We further examined the expression of *SALL4*, *EPCAM*, and *AFP* using microarray data of 238 HCC cases (Fig. 1E) and qRT-PCR data of 61 HCC cases (Fig. 1F). For the tumor/non-tumor ratios, we identified a weak positive correlation between *SALL4* and *EPCAM* (r = 0.31, $p < 0.0001$) and between *SALL4* and *AFP* (r = 0.31, $p = 0.0003$) in the microarray cohort. We further evaluated expression of these genes in HCC tissues by qRT-PCR, and we validated the strong positive correlation between *SALL4* and *EPCAM* (r = 0.70, $p < 0.0001$) and between *SALL4* and AFP (r = 0.66, $p < 0.0001$) in the independent cohort.

Next we performed IHC analysis of 144 HCC cases surgically resected at Kanazawa University Hospital. We first confirmed the nuclear accumulation of SALL4 stained by an anti-human SALL4 antibody (Fig. 2A). We further confirmed the concordance of SALL4 protein expression evaluated by IHC, and *SALL4* gene expression evaluated by qRT-PCR using the same samples (Fig. 2B). We detected the nuclear expression of SALL4 in 43 of 144 HCC cases (Table 1). After evaluating the clinicopathological characteristics of SALL4-positive and -negative HCC cases, we identified that SALL4-positive HCCs were associated with a significantly high frequency of hepatitis B virus (HBV) infection and significantly high serum AFP values. We further identified that

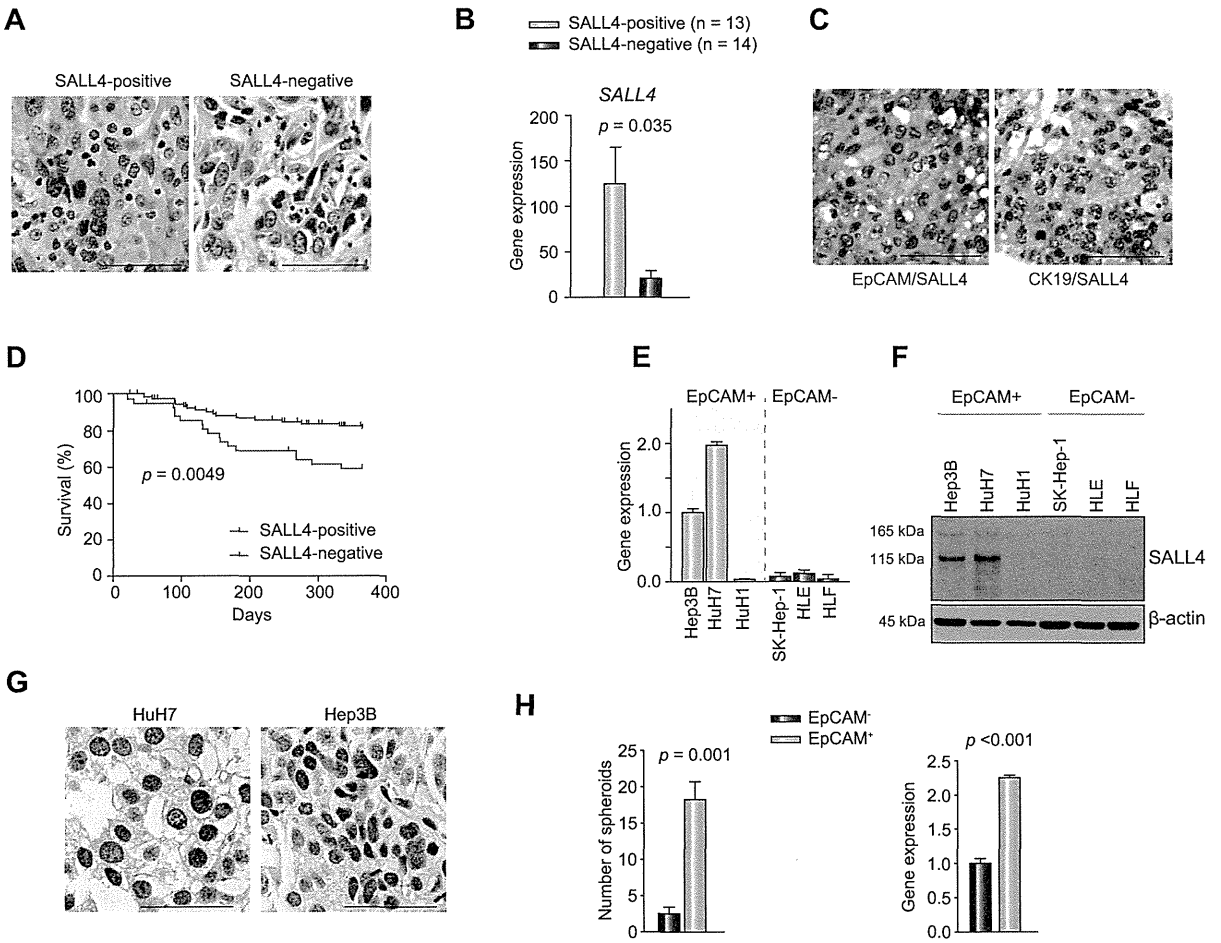

Fig. 2. SALL4 expression in human primary HCCs and cell lines. (A) Representative images of SALL4-positive and -negative HCC immunostaining (scale bar, 100 μm). (B) Gene expression of *SALL4* in SALL4-positive (n = 13) and -negative HCCs (n = 14) as shown by IHC (mean ± SD). (C) Double color IHC analysis of HCC stained with anti-SALL4 and anti-EpCAM or anti-CK19 antibodies (scale bar, 100 μm). (D) Kaplan-Meier survival analysis with Log-rank. Recurrence-free survival of SALL4-positive (n = 43) and -negative (n = 101) HCCs was analyzed. (E) *SALL4* expression in EpCAM$^+$ (Hep3B, HuH7, and HuH1) and EpCAM$^-$ (SK-Hep-1, HLE, and HLF) HCC cell lines evaluated by qRT-PCR. (F) SALL4 expression in EpCAM$^+$ and EpCAM$^-$ HCC cell lines evaluated by Western blotting. (G) IHC analysis of SALL4 expression in subcutaneous tumors obtained from EpCAM$^+$ (HuH7 and Hep3B) HCC cell lines xenografted in NOD/SCID mice. (H) Spheroid formation capacity of sorted EpCAM$^+$ and EpCAM$^-$ cells obtained from a primary HCC. Number of spheroids obtained from 2000 sorted cells is indicated (n = 3, mean ± SD). Gene expression of *SALL4* in sorted EpCAM$^+$ and EpCAM$^-$ cells obtained from a primary HCC (n = 3, mean ± SD). (This figure appears in colour on the web.)

SALL4-positive HCCs were associated with expression of the hepatic stem cell markers EpCAM and CK19. Co-expression of SALL4, EpCAM, and CK19 was confirmed by double color IHC analysis (Fig. 2C). Evaluation of the survival outcome of these surgically resected HCC cases by Kaplan-Meier survival analysis indicated that SALL4-positive HCCs were associated with significantly lower recurrence-free survival outcomes within one year compared with SALL4-negative HCCs ($p = 0.0049$) (Fig. 2D).

Because SALL4 expression was positively correlated with EpCAM and AFP expression in primary HCC cases, we evaluated the expression of SALL4 in EpCAM$^+$ AFP$^+$ and EpCAM$^-$ AFP$^-$ HCC cell lines. Consistent with the primary HCC data, two of three EpCAM$^+$ AFP$^+$ HCC cell lines (Hep3B and HuH7) abundantly expressed SALL4, as shown by qRT-PCR (Fig. 2E) and Western blotting (Fig. 2F). We identified the expression of two isoforms of SALL4 proteins with molecular weights of 165 kDa (SALL4A) and 115 kDa (SALL4B), and SALL4B was found to be the dominant endogenous isoform in HCC cell lines. All EpCAM$^-$ AFP$^-$ HCC cell lines (SK-Hep-1, HLE, and HLF) and one EpCAM$^+$ AFP$^+$ cell line (HuH1) did not express SALL4. Nuclear accumulation of SALL4 in Hep3B and HuH7 cells was confirmed by IHC using subcutaneous tumors developed in xenotransplanted NOD/SCID mice (Fig. 2G). We further evaluated the expression of *EPCAM* and *SALL4* using single cell suspensions derived from a surgically resected primary HCC. EpCAM$^+$ and EpCAM$^-$ cells were separated by magnetic beads, and we revealed a strong spheroid formation capacity of sorted EpCAM$^+$ cells compared with EpCAM$^-$ cells (Fig. 2H, left panel). Interestingly, when comparing the expression of *SALL4* in these sorted cells, we identified a high expression of *SALL4* in sorted EpCAM$^+$ cells compared with EpCAM$^-$ cells (Fig. 2H, right panel), indicating that *SALL4* is activated in EpCAM$^+$ liver CSCs.

Table 1. Clinicopathological characteristics of SALL4-positive and -negative HCC cases used for IHC analyses.

Parameters	SALL4-positive (n = 43)	SALL4-negative (n = 101)	*p* value*
Age (yr, mean ± SE)	60.8 ± 1.8	64.6 ± 1.0	0.13
Sex (male/female)	27/16	70/18	0.06
Etiology (HBV/HCV/B + C/other)	21/14/0/8	20/63/3/15	0.0014
Liver cirrhosis (yes/no)	21/22	61/40	0.27
AFP (ng/ml, mean ± SE)	13,701 ± 9292	175.5 ± 55.0	<0.0001
Histological grade**			
I-II	3	18	
II-III	33	68	
III-IV	7	15	0.24
Tumor size (<3 cm/>3 cm)	17/26	57/44	0.071
EpCAM (positive/negative)	27/16	29/72	0.0002
CK19 (positive/negative)	12/31	12/89	0.027

*Mann-Whitney U-test or χ^2 test.
**Edmondson-Steiner.

SALL4 regulates stemness of HpSC-HCC

To explore the role of SALL4 in HpSC-HCC, we evaluated the effect of its overexpression in HuH1 cells which showed little expression of SALL4 irrespective of $EpCAM^+$ and AFP^+ HpSC-HCC phenotype. We transfected plasmid constructs encoding SALL4 (pCMV6-SALL4) or control (pCMV7), and we similarly identified the expression of two isoforms by using this construct (Fig. 3A). Evaluation of the subcellular localization of GFP-tagged SALL4 (pCMV6-SALL4-GFP) showed that it could be detected in both the cytoplasm and nucleus (Fig. 3B). We observed strong up-regulation of the hepatic stem cell marker *KRT19*, modest up-regulation of *EPCAM* and *CD44*, and down-regulation of the mature hepatocyte marker *ALB* in HuH1 cells transfected with pCMV6-SALL4 compared with the control (Fig. 3C). Up-regulation of CK19 by SALL4 overexpression was also confirmed at the protein level by IF analysis (Fig. 3D). Phenotypically, SALL4 overexpression in HuH1 cells resulted in the significant activation of spheroid formation and invasion capacities with activation of *SNAI1*, which induces epithelial-mesenchymal transition, compared with the control (Fig. 3E and F, Supplementary Fig. 1A).

We further investigated the effect of SALL4 knockdown in HuH7 cells, which intrinsically expressed high levels of SALL4. Expression of *SALL4* was decreased to 50% in HuH7 cells transfected with SALL4 sh-RNA compared with the control when evaluated by qRT-PCR (Fig. 4A). However, the reduction of SALL4 protein was more evident when evaluated by Western blotting, suggesting that this sh-RNA construct might work at the translational as well as the transcriptional level (Fig. 4B). Knock down of *SALL4* resulted in a compromised invasion capacity and spheroid formation capacity with decreased expression of *EPCAM* and *CD44* in HuH7 cells (Fig. 4C and D, Supplementary Fig. 1B and C).

SALL4 and HDAC activity in HpSC-HCC

The above data suggested that SALL4 is a good target and biomarker for the diagnosis and treatment of HpSC-HCCs. However, it is difficult to directly target SALL4 as no studies have investigated the inhibition of its transcription using chemical or other approaches [21]. We therefore re-investigated the interaction networks associated with *SALL4*, and found that SALL4 activation appeared to induce epigenetic modification (Fig. 1B). In particular, a recent study suggested that SALL4 forms a nucleosome remodeling and deacetylase (NuRD) complex with HDACs and potentially regulates HDAC activity [22]. We therefore confirmed that *SALL4* knock down resulted in the reduced activity of total HDAC in HuH7 cells (Fig. 4E). We also evaluated the effect of the overexpression of SALL4 in HuH1 and HLE cells, which do not express SALL4 endogenously, and SALL4 overexpression was found to result in a modest increase of HDAC activity and mild enhancement of chemosensitivity to an HDAC inhibitor SBHA in both cell lines (Supplementary Fig. 2A and B). We further investigated HDAC activity in two SALL4-positive (Hep3B, HuH7) and two SALL4-negative (HLE, HLF) HCC cell lines. Interestingly, high HDAC activities were detected in SALL4-positive compared with SALL4-negative HCC cell lines (Fig. 4F). The HDAC inhibitor SBHA was found to inhibit proliferation of SALL4-positive HCC cell lines at a concentration of 10 μM. By contrast, SBHA had little effect on the proliferation of SALL4-negative HCC cell lines at this concentration (Fig. 4G). SBHA treatment suppressed the expression of SALL4 gene/protein expression in SALL4-positive HuH7 and Hep3B cell lines (Supplementary Fig. 3A and B). We further investigated the effect of SAHA, an additional HDAC inhibitor, in these HCC cell lines, and SAHA was found to more efficiently suppress the cell proliferation of SALL4-positive cell lines compared with SALL4-negative cell lines (Supplementary Fig. 3C).

Taken together, our data suggest a pivotal role for the transcription factor SALL4 in regulating the stemness of HpSC-HCC. SALL4 was detected in HpSC-HCCs with poor prognosis, and inactivation of SALL4 resulted in a reduced invasion/spheroid formation capacity and decreased expression of hepatic stem cell markers. The HDAC inhibitors inhibited proliferation of SALL4-positive HCC cell lines with a reduction of SALL4 gene/protein expression, suggesting their potential in the treatment of SALL4-positive HpSC-HCC.

Discussion

Stemness traits in cancer cells are currently of great interest because they may explain the clinical outcome of patients according to the malignant nature of their tumor. Recently, we

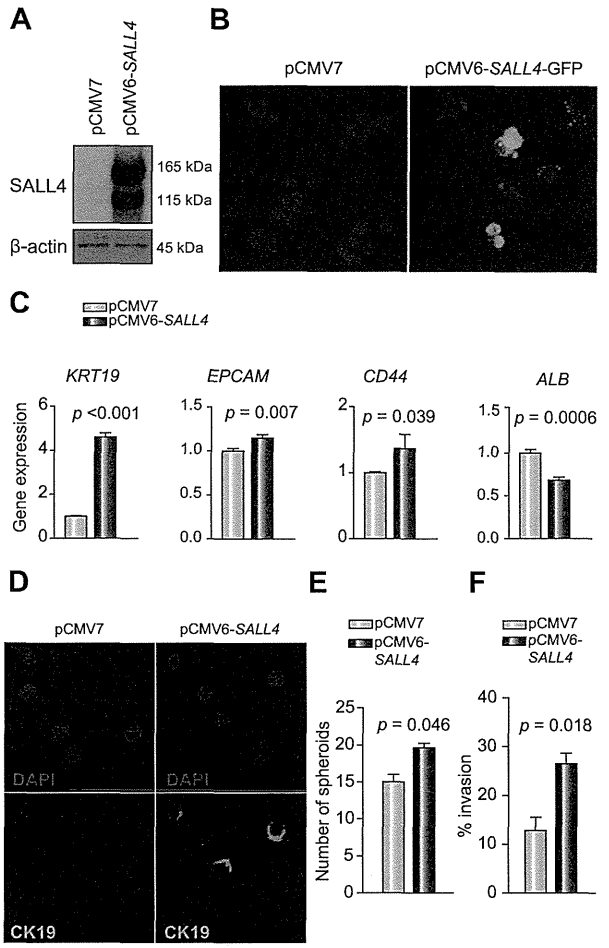

Fig. 3. Effect of SALL4 overexpression. (A) Western blots of cell lysates with anti-SALL4 antibodies. HuH1 cells were transfected with pCMV7 or pCMV6-*SALL4* and incubated for 72 h. (B) IF analysis of HuH1 cells transfected with pCMV7 or pCMV6-*SALL4* and incubated for 72 h. (C) qRT-PCR analysis of *KRT19*, *EPCAM*, *CD44*, and *ALB* in HuH1 cells transfected with pCMV7 or pCMV6-*SALL4* and incubated for 48 h. (D) IF analysis of HuH1 cells transfected with pCMV7 or pCMV6-*SALL4*, incubated for 72 h and stained with anti-CK19 antibodies, evaluated by the confocal laser scanning microscopy. (E) Spheroid formation assay of HuH1 cells transfected with pCMV7 or pCMV6-*SALL4*. Number of spheroids obtained from 2000 cells is indicated (n = 3, mean ± SD). (F) Invasion assay of HuH1 cells transfected with pCMV7 or pCMV6-*SALL4* (n = 3, mean ± SD). (This figure appears in colour on the web.)

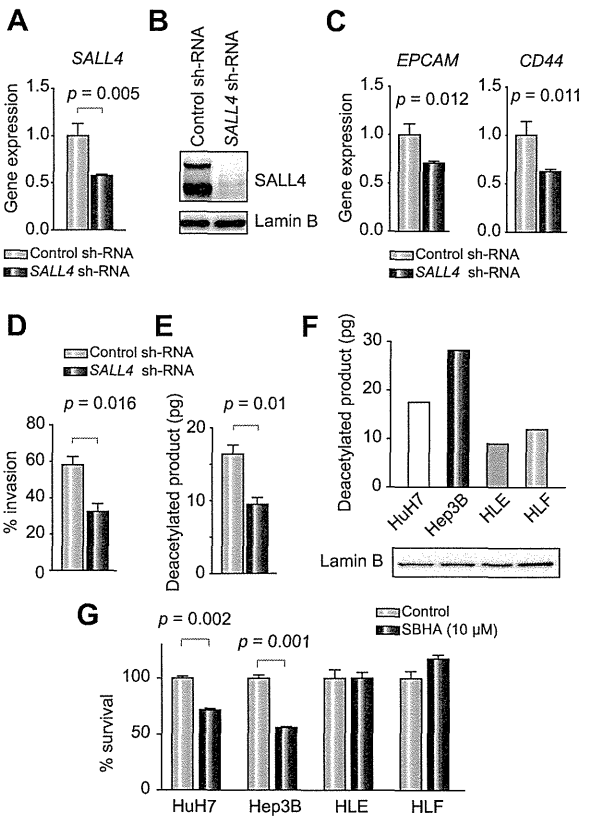

Fig. 4. Effect of *SALL4* knockdown and HDAC activity. (A) qRT-PCR analysis of *SALL4* in HuH7 cells transfected with control or *SALL4* sh-RNAs (n = 3, mean ± SD). (B) Western blots of lysates obtained from HuH7 cells transfected with control or *SALL4* sh-RNAs with anti-SALL4 antibodies. (C) qRT-PCR analysis of *EPCAM* and *CD44* in HuH7 cells transfected with control or *SALL4* sh-RNAs (n = 3, mean ± SD). (D) Invasion assay of HuH7 cells transfected with control or *SALL4* sh-RNAs (n = 3, mean ± SD). (E) HDAC activity of nuclear extracts obtained from HuH7 cells transfected with control or *SALL4* sh-RNAs. (F) HDAC activity of nuclear extracts obtained from each cell line. HDAC activity was measured in duplicate and average amounts of deacetylated products are indicated (upper panel). Lamin B included in the nuclear extracts loaded for HDAC activity assays was measured by Western blotting (lower panel). (G) Cell proliferation assay of HCC cell lines. Each cell line was treated with control DMSO or 10 μM SBHA and cultured for 72 h (n = 4, mean ± SD).

proposed an HCC classification system based on the stem/maturation status of the tumor by EpCAM and AFP expression status [8]. These HCC subtypes showed distinct gene expression patterns with features resembling particular stages of liver lineages. Among them, HpSC-HCC was characterized by a highly invasive nature, chemoresistance to fluorouracil, and poor prognosis after radical resection, warranting the development of a novel therapeutic approach against this HCC subtype [9].

In this study, we showed that the transcription factor SALL4 was activated in HpSC-HCC and that SALL4 might regulate HCC stemness, as characterized by the activation of EpCAM, CK19, and CD44 with highly tumorigenic and invasive natures. Furthermore, we identified that SALL4-positive HCC cell lines tended to show high HDAC activity and chemosensitivity to the HDAC inhibitors SBHA and SAHA. This study reveals for the first time the utility of SBHA for the treatment of HCC with stem cell features.

SALL4 is a zinc finger transcription factor originally cloned based on sequence homology to *Drosophila sal* [11]. *SALL4* mutations are associated with the Okihiro syndrome, a human disease involving multiple organ defects [23,24]. SALL4 plays a fundamental role in the maintenance of embryonic stem cells, potentially through interaction with Oct4, Sox2, and Nanog [25–30]. Furthermore, knockdown of SALL4 significantly reduces the efficiency of induced pluripotent stem cell generation [31]. *SALL4* is also expressed in hematopoietic stem cells and leukemia cells, where it regulates their maintenance [14,32]. SALL4 is known to encode two isoforms (*SALL4A* and *SALL4B*), and a recent study

suggested the important role of SALL4B on maintaining the stemness of embryonic stem cells [25]. Interestingly, our data indicated that SALL4B is also a dominant form in HpSC-HCC cell lines. It is unclear how SALL4 isoform expression is regulated in cancer, and future studies are required to explore the mechanisms of SALL4 isoform regulation.

In the liver, SALL4 is expressed in fetal hepatic stem/progenitors but not in adult hepatocytes, and a mouse study demonstrated that inhibition of SALL4 in hepatic stem/progenitors contributes to their differentiation [33]. Interestingly, recent studies indicated that AFP-producing gastric cancer expresses SALL4, suggesting that SALL4 might play a role in the hepatoid differentiation of gastric cancer [34]. Consistently, our data indicated a positive correlation between *SALL4*, *AFP*, and *EPCAM* expression in two independent HCC cohorts. Strikingly, SALL4 was recently shown to be expressed in a subset of human liver cancers with poor prognoses, while modification of SALL4 expression resulted in the alteration of cell proliferation *in vitro* and tumor growth *in vivo*, consistent with our current study [35]. A recent study reported the expression of SALL4 in 46% of HCC cases, which is almost comparable to our present study [36]. Furthermore, a very recent study of two independent large cohorts demonstrated that SALL4 is a marker for a progenitor subclass of HCC with an aggressive phenotype [37]. It is still unclear how SALL4 expression is regulated and which target genes are directly activated by SALL4 binding. Future studies using next generation sequencing are required to fully understand the mechanisms of SALL4 regulation of HCC stemness.

In this study, we demonstrated that SALL4-positive HCC cell lines have high HDAC activity and chemosensitivity against the HDAC inhibitors SBHA and SAHA compared with SALL4-negative HCC cell lines. SALL4 was recently found to directly connect with the epigenetic modulator NuRD complex [22], thereby possibly affecting the histone modification associated with stemness. The NuRD complex is a multiunit chromatin remodeling complex containing chromodomain-helicase-DNA-binding proteins and HDACs that regulate histone deacetylation [38]. Its role in cancer is still controversial, while its function in HCC has not yet been determined.

Our data suggest that SALL4 plays a role in controlling HDAC activity and contributing to the maintenance of HCC with stem cell features. Consistently, HDAC inhibitors might be useful for the eradication of SALL4-positive HCC cells through their inhibitory effects on histone deacetylation by NuRD [39]. Encouragingly, a recent study demonstrated the utility of a SALL4-binding peptide to inhibit its binding to phosphatase and tensin homolog deleted on chromosome 10 (PTEN) through interaction with HDAC, thereby targeting leukemia cells [21]. Further studies are required to understand the relationship between SALL4, the NuRD complex, and the maintenance of stemness in HCC.

Financial support

This study was supported by a Grant-in-Aid from the Ministry of Education, Culture, Sports, Science and Technology, Japan (23590967), a grant from the Japanese Society of Gastroenterology, a grant from the Ministry of Health, Labour and Welfare, and a grant from the National Cancer Center Research and Development Fund (23-B-5), Japan.

Conflict of interest

The authors who have taken part in this study declared that they do not have anything to disclose regarding funding or conflict of interest with respect to this manuscript.

Acknowledgments

We thank Ms. Masayo Baba and Ms. Nami Nishiyama for excellent technical assistance.

Supplementary data

Supplementary data associated with this article can be found, in the online version, at http://dx.doi.org/10.1016/j.jhep.2013.08.024.

References

[1] Nowell PC. The clonal evolution of tumor cell populations. Science 1976;194:23–28.
[2] Hanahan D, Weinberg RA. Hallmarks of cancer: the next generation. Cell 2011;144:646–674.
[3] Jordan CT, Guzman ML, Noble M. Cancer stem cells. N Engl J Med 2006;355:1253–1261.
[4] Clarke MF, Dick JE, Dirks PB, Eaves CJ, Jamieson CH, Jones DL, et al. Cancer stem cells–perspectives on current status and future directions: AACR Workshop on cancer stem cells. Cancer Res 2006;66:9339–9344.
[5] Dean M, Fojo T, Bates S. Tumour stem cells and drug resistance. Nat Rev Cancer 2005;5:275–284.
[6] Visvader JE, Lindeman GJ. Cancer stem cells in solid tumours: accumulating evidence and unresolved questions. Nat Rev Cancer 2008;8:755–768.
[7] Jemal A, Bray F, Center MM, Ferlay J, Ward E, Forman D. Global cancer statistics. CA Cancer J Clin 2011;61:69–90.
[8] Yamashita T, Forgues M, Wang W, Kim JW, Ye Q, Jia H, et al. EpCAM and alpha-fetoprotein expression defines novel prognostic subtypes of hepatocellular carcinoma. Cancer Res 2008;68:1451–1461.
[9] Yamashita T, Ji J, Budhu A, Forgues M, Yang W, Wang HY, et al. EpCAM-positive hepatocellular carcinoma cells are tumor-initiating cells with stem/progenitor cell features. Gastroenterology 2009;136:1012–1024.
[10] Yamashita T, Budhu A, Forgues M, Wang XW. Activation of hepatic stem cell marker EpCAM by Wnt-beta-catenin signaling in hepatocellular carcinoma. Cancer Res 2007;67:10831–10839.
[11] de Celis JF, Barrio R. Regulation and function of spalt proteins during animal development. Int J Dev Biol 2009;53:1385–1398.
[12] Aguila JR, Liao W, Yang J, Avila C, Hagag N, Senzel L, et al. SALL4 is a robust stimulator for the expansion of hematopoietic stem cells. Blood 2011;118:576–585.
[13] Yang J, Chai L, Gao C, Fowles TC, Alipio Z, Dang H, et al. SALL4 is a key regulator of survival and apoptosis in human leukemic cells. Blood 2008;112:805–813.
[14] Yang J, Chai L, Liu F, Fink LM, Lin P, Silberstein LE, et al. Bmi-1 is a target gene for SALL4 in hematopoietic and leukemic cells. Proc Natl Acad Sci U S A 2007;104:10494–10499.
[15] Yamashita T, Honda M, Nio K, Nakamoto Y, Takamura H, Tani T, et al. Oncostatin m renders epithelial cell adhesion molecule-positive liver cancer stem cells sensitive to 5-fluorouracil by inducing hepatocytic differentiation. Cancer Res 2010;70:4687–4697.
[16] Yamashita T, Honda M, Takatori H, Nishino R, Minato H, Takamura H, et al. Activation of lipogenic pathway correlates with cell proliferation and poor prognosis in hepatocellular carcinoma. J Hepatol 2009;50:100–110.
[17] Woo HG, Wang XW, Budhu A, Kim YH, Kwon SM, Tang ZY, et al. Association of TP53 mutations with stem cell-like gene expression and survival of patients with hepatocellular carcinoma. Gastroenterology 2011;140:1063–1070.
[18] Ji J, Wang XW. Clinical implications of cancer stem cell biology in hepatocellular carcinoma. Semin Oncol 2012;39:461–472.

[19] Yang J, Corsello TR, Ma Y. Stem cell gene SALL4 suppresses transcription through recruitment of DNA methyltransferases. J Biol Chem 2012;287: 1996–2005.
[20] Bohm J, Sustmann C, Wilhelm C, Kohlhase J. SALL4 is directly activated by TCF/LEF in the canonical Wnt signaling pathway. Biochem Biophys Res Commun 2006;348:898–907.
[21] Gao C, Dimitrov T, Yong KJ, Tatetsu H, Jeong HW, Luo HR, et al. Targeting transcription factor SALL4 in acute myeloid leukemia by interrupting its interaction with an epigenetic complex. Blood 2013;121:1413–1421.
[22] Lu J, Jeong HW, Kong N, Yang Y, Carroll J, Luo HR, et al. Stem cell factor SALL4 represses the transcriptions of PTEN and SALL1 through an epigenetic repressor complex. PLoS One 2009;4:e5577.
[23] Al-Baradie R, Yamada K, St Hilaire C, Chan WM, Andrews C, McIntosh N, et al. Duane radial ray syndrome (Okihiro syndrome) maps to 20q13 and results from mutations in SALL4, a new member of the SAL family. Am J Hum Genet 2002;71:1195–1199.
[24] Kohlhase J, Heinrich M, Schubert L, Liebers M, Kispert A, Laccone F, et al. Okihiro syndrome is caused by SALL4 mutations. Hum Mol Genet 2002;11:2979–2987.
[25] Rao S, Zhen S, Roumiantsev S, McDonald LT, Yuan GC, Orkin SH. Differential roles of Sall4 isoforms in embryonic stem cell pluripotency. Mol Cell Biol 2010;30:5364–5380.
[26] Tanimura N, Saito M, Ebisuya M, Nishida E, Ishikawa F. Stemness-related factor sall4 interacts with transcription factors oct-3/4 and sox2 and occupies oct-sox elements in mouse embryonic stem cells. J Biol Chem 2013;288:5027–5038.
[27] Wu Q, Chen X, Zhang J, Loh YH, Low TY, Zhang W, et al. Sall4 interacts with nanog and co-occupies nanog genomic sites in embryonic stem cells. J Biol Chem 2006;281:24090–24094.
[28] Yang J, Chai L, Fowles TC, Alipio Z, Xu D, Fink LM, et al. Genome-wide analysis reveals Sall4 to be a major regulator of pluripotency in murine-embryonic stem cells. Proc Natl Acad Sci U S A 2008;105:19756–19761.
[29] Yang J, Gao C, Chai L, Ma Y. A novel SALL4/OCT4 transcriptional feedback network for pluripotency of embryonic stem cells. PLoS One 2010;5:e10766.
[30] Zhang J, Tam WL, Tong GQ, Wu Q, Chan HY, Soh BS, et al. Sall4 modulates embryonic stem cell pluripotency and early embryonic development by the transcriptional regulation of Pou5f1. Nat Cell Biol 2006;8:1114–1123.
[31] Tsubooka N, Ichisaka T, Okita K, Takahashi K, Nakagawa M, Yamanaka S. Roles of Sall4 in the generation of pluripotent stem cells from blastocysts and fibroblasts. Genes Cells 2009;14:683–694.
[32] Yang J, Liao W, Ma Y. Role of SALL4 in hematopoiesis. Curr Opin Hematol 2012;19:287–291.
[33] Oikawa T, Kamiya A, Kakinuma S, Zeniya M, Nishinakamura R, Tajiri H, et al. Sall4 regulates cell fate decision in fetal hepatic stem/progenitor cells. Gastroenterology 2009;136:1000–1011.
[34] Ikeda H, Sato Y, Yoneda N, Harada K, Sasaki M, Kitamura S, et al. Alpha-Fetoprotein-producing gastric carcinoma and combined hepatocellular and cholangiocarcinoma show similar morphology but different histogenesis with respect to SALL4 expression. Hum Pathol 2012;43:1955–1963.
[35] Oikawa T, Kamiya A, Zeniya M, Chikada H, Hyuck AD, Yamazaki Y, et al. SALL4, a stem cell biomarker in liver cancers. Hepatology 2013;57:1469–1483.
[36] Gonzalez-Roibon N, Katz B, Chaux A, Sharma R, Munari E, Faraj SF, et al. Immunohistochemical expression of SALL4 in hepatocellular carcinoma, a potential pitfall in the differential diagnosis of yolk sac tumors. Hum Pathol 2013;44:1293–1299.
[37] Yong KJ, Gao C, Lim JS, Yan B, Yang H, Dimitrov T, et al. Oncofetal gene SALL4 in aggressive hepatocellular carcinoma. N Engl J Med 2013;368: 2266–2276.
[38] Lai AY, Wade PA. Cancer biology and NuRD: a multifaceted chromatin remodelling complex. Nat Rev Cancer 2011;11:588–596.
[39] Marquardt JU, Thorgeirsson SS. Sall4 in "stemness"-driven hepatocarcinogenesis. N Engl J Med 2013;368:2316–2318.

PLOS | ONE

microRNA-122 Abundance in Hepatocellular Carcinoma and Non-Tumor Liver Tissue from Japanese Patients with Persistent HCV versus HBV Infection

Carolyn Spaniel[1,2], Masao Honda[3], Sara R. Selitsky[1,4], Daisuke Yamane[1], Tetsuro Shimakami[3], Shuichi Kaneko[3], Robert E. Lanford[5], Stanley M. Lemon[1*]

1 Departments of Medicine and Microbiology & Immunology and the Lineberger Comprehensive Cancer Center, the University of North Carolina at Chapel Hill, Chapel Hill, North Carolina, United States of America, **2** Department of Microbiology and Immunology, University of Texas Medical Branch, Galveston, Texas, United States of America, **3** Department of Gastroenterology, Kanazawa University Graduate School of Medicine, Takara-Machi, Kanazawa, Japan, **4** Department of Genetics, the University of North Carolina at Chapel Hill, Chapel Hill, North Carolina, United States of America, **5** Department of Virology and Immunology, Texas Biomedical Research Institute, San Antonio, Texas, United States of America

Abstract

Mechanisms of hepatic carcinogenesis in chronic hepatitis B and hepatitis C are incompletely defined but often assumed to be similar and related to immune-mediated inflammation. Despite this, several studies hint at differences in expression of miR-122, a liver-specific microRNA with tumor suppressor properties, in hepatocellular carcinoma (HCC) associated with hepatitis B virus (HBV) versus hepatitis C virus (HCV) infection. Differences in the expression of miR-122 in these cancers would be of interest, as miR-122 is an essential host factor for HCV but not HBV replication. To determine whether the abundance of miR-122 in cancer tissue is influenced by the nature of the underlying virus infection, we measured miR-122 by qRT-PCR in paired tumor and non-tumor tissues from cohorts of HBV- and HCV-infected Japanese patients. miR-122 abundance was significantly reduced from normal in HBV-associated HCC, but not in liver cancer associated with HCV infection. This difference was independent of the degree of differentiation of the liver cancer. Surprisingly, we also found significant differences in miR-122 expression in non-tumor tissue, with miR-122 abundance reduced from normal in HCV- but not HBV-infected liver. Similar differences were observed in HCV- vs. HBV-infected chimpanzees. Among HCV-infected Japanese subjects, reductions in miR-122 abundance in non-tumor tissue were associated with a single nucleotide polymorphism near the IL28B gene that predicts poor response to interferon-based therapy (TG vs. TT genotype at rs8099917), and correlated negatively with the abundance of multiple interferon-stimulated gene transcripts. Reduced levels of miR-122 in chronic hepatitis C thus appear to be associated with endogenous interferon responses to the virus, while differences in miR-122 expression in HCV- versus HBV-associated HCC likely reflect virus-specific mechanisms contributing to carcinogenesis. The continued expression of miR-122 in HCV-associated HCC may signify an important role for HCV replication late in the progression to malignancy.

Citation: Spaniel C, Honda M, Selitsky SR, Yamane D, Shimakami T, et al. (2013) microRNA-122 Abundance in Hepatocellular Carcinoma and Non-Tumor Liver Tissue from Japanese Patients with Persistent HCV versus HBV Infection. PLoS ONE 8(10): e76867. doi:10.1371/journal.pone.0076867

Editor: Birke Bartosch, Inserm, U1052, UMR 5286, France

Received May 19, 2013; **Accepted** August 29, 2013; **Published** October 9, 2013

Funding: This work was supported in part by National Institutes of Health grants R01-AI095690 and R01-CA164029 and the University Cancer Research Fund. The funders had no role in study design, data collection and analysis, decision to publish, or preparation of the manuscript.

Competing interests: The authors have declared that no competing interests exist.

* E-mail: smlemon@med.unc.edu

Introduction

Globally, liver cancer is the fifth and seventh most common malignancy in men and women, respectively, and the third most deadly [1]. Most (85-95%) of these cancers are hepatocellular carcinoma (HCC) [2], and many are associated with persistent intrahepatic infections with hepatitis C virus (HCV) or hepatitis B virus (HBV) [2,3]. Although the total cancer death rate decreased within the United States by over 1.5% between 2001-2007, deaths due to liver cancer increased by 50% among males and by 29% in females [4]. These changes in the incidence of HCC are largely due to increases in HCV-associated malignancy. Similarly, while HBV infection historically has been the major risk factor underlying development of HCC in Asia, in Japan it has been supplanted in recent decades by HCV infection [5].

The exact mechanisms underlying HCV- and HBV-associated malignancy are unknown [6,7]. Chronic infections with either virus may result in cirrhosis, which alone is a major risk factor for liver cancer [2]. However, there may also be

virus-specific mechanisms at work. While immune-mediated mechanisms are both necessary and sufficient for the development of HBV-related cancer in murine models, liver cancer arises in the absence of inflammation in HCV-transgenic mice [8,9]. Moreover, some HCV proteins may interact with host tumor suppressors and possibly impair cellular responses to DNA damage [10]. If virus-specific mechanisms of oncogenesis are important in the development of HCC, it is reasonable to anticipate that the pathways leading to HCV- and HBV-associated cancer might differ, possibly leaving distinguishing genetic or epigenetic marks in the tumors that arise. If so, understanding these differences would be important for biomarker discovery, and potentially design of preventative and therapeutic interventions.

Here, we describe a study that was aimed at determining whether the abundance of microRNA-122 (miR-122) is different in liver cancer arising in patients with chronic HCV infection compared to cancers arising in the context of chronic HBV infection. Mature microRNAs (miRNAs) are 20-23 nucleotides in length and encoded either by microRNA genes or from within conventional protein-coding genes. They act generally by binding to specific sites within the 3' untranslated region (3' UTR) of cellular mRNAs, to which they recruit RNA-induced silencing complexes (RISC) that repress translation and destabilize the mRNA [11–13]. miR-122 is a liver-specific miRNA that accounts for the majority of miRNAs in hepatocytes [14]. It regulates a large number of genes within the liver [15], and has several tumor suppressor-like properties [16,17]. Importantly, miR-122 is a crucial host factor for HCV replication, binding to the 5' untranslated RNA segment of the viral genome, physically stabilizing it, and promoting viral protein expression [18–20].

Because of its liver-specific nature and tumor suppressor-like qualities [16,17], it is of interest to know whether miR-122 expression is altered in liver cancers. Prior studies investigating miR-122 expression in liver cancers have produced conflicting results, particularly as related to the underlying viral causes of cancer. Two early studies suggest that miR-122 abundance is generally reduced in HCC [21,22]. However, Hou et al. [23] reported that miR-122 expression was maintained in both HBV- and HCV-associated cancer, while Varnholt et al. [24] reported that miR-122 levels were increased significantly in HCV-associated cancers when compared to non-cancerous tissue. Coulouarn et al. [25] reported higher miR-122 expression levels in HCV- versus HBV-associated cancers. To some extent, these conflicting results may reflect different patient populations, or possibly methodologic differences, not only in the measurement of miR-122 abundance but also in how miR-122 abundance was compared across tissue samples.

In an effort to resolve this controversy, we conducted a comprehensive analysis of miR-122 expression in liver cancers arising in a genetically homogenous group of Japanese patients. Using a highly accurate, miR-122-specific quantitative reverse-transcription, polymerase chain reaction (qRT-PCR) assay, and paying particular attention to how miR-122 measurements are compared between tissue samples, we show that miR-122 expression is significantly reduced in HBV-associated HCC but not in most HCV-associated cancers. We also demonstrate that miR-122 abundance is reduced in non-tumor HCV-infected liver in association with increased expression of interferon (IFN)-stimulated genes (ISGs).

Materials and Methods

Ethics statement

Liver tissue was obtained from Japanese patients undergoing surgical resection of liver cancer (primary or metastatic) at the Liver Center of Kanazawa University Hospital (Kanazawa, Japan). All subjects provided written informed consent for participation in the study, and tissue acquisition procedures were approved by the ethics committee of Kanazawa University under a protocol entitled "Gene expression analysis of peripheral blood cells and liver in patients with liver and gastrointestinal cancers". Archived liver tissue and serum samples were collected prior to December 15, 2011 from chimpanzees housed and cared for at the Southwest National Primate Research Center (SNPRC) of the Texas Biomedical Research Institute in accordance with the Guide for the Care and Use of Laboratory Animals. All protocols were approved by the Institutional Animal Care and Use Committee. SNPRC is accredited by the Association for Assessment and Accreditation of Laboratory Animal Care (AAALAC) International and operates in accordance with the NIH and U.S. Department of Agriculture guidelines and the Animal Welfare Act.

Human subjects and tissue samples

Paired samples of HCC and non-tumor liver tissue were obtained from Japanese patients undergoing surgical resection of HCC at the Liver Center of Kanazawa University Hospital (Kanazawa, Japan). Non-infected 'normal' liver tissue was similarly collected from patients undergoing resection of metastases of non-hepatic primary cancers. Patients were categorized as HCV-infected by the presence of HCV RNA (COBAS Ampli-Prep/COBAS TaqMan System) and absence of hepatitis B surface antigen (HBsAg) in serum or plasma at the time of surgery, while HBV infection was defined by the presence of HBsAg and absence of anti-HCV antibodies. HCC was categorized according to the degree of cellular differentiation, while fibrosis and inflammation in non-tumor tissue from HBV- and HCV-infected patients were compared after scoring each [26,27]. The IL28B genotype of study subjects with HCV infection was defined at the rs8099917 locus as described previously [28].

Chimpanzee care and sample collection

We studied archived liver tissue and serum samples collected prior to December 15, 2011 from chimpanzees housed and cared for at the Southwest National Primate Research Center (SNPRC) of the Texas Biomedical Research Institute. At the time samples were obtained, animals considered to be non-infected ('normal') were negative for HBV and HCV markers; HBV infection was defined as the presence of serum HBsAg, and HCV infection by the presence of HCV RNA detectable in sera by RT-PCR.

Small RNA quantitation in human samples

Human tissue samples were stored in liquid nitrogen until processed for RNA extraction. Approximately 1 mg of tissue was ground using a tissue homogenizer and total RNA isolated using the mirVana miRNA isolation kit (Ambion). Liver RNA samples were subsequently stored at -80°C or on dry ice during shipment. The quality of the isolated RNA (RIN score) was assessed using an Agilent 2100 Bioanalyzer (Agilent RNA 6000 Nano Kit, Agilent Technologies) [29]. Quantification of miR-122, miR-191, Let-7a, miR-24, and the small nuclear RNA (snRNA) U6 was carried out by quantitative reverse-transcription, polymerase chain reaction (qRT-PCR) in a two-step process. RNA (12.5 ng) was reversed transcribed in a 10 µl reaction mix using reagents provided with the Universal cDNA Synthesis kit (Exiqon) and the manufacturer's recommended procedure. Quantitative PCR was carried out subsequently with the SYBR Green Master Mix Kit (Exiqon), mixed locked-nucleic acid primer sets specific for each miRNA or snRNA (Exiqon), and the CFX96 PCR System (Bio-Rad). Results are presented as relative copy number normalized to total RNA. Alternatively, absolute miR-122 copy numbers were estimated using serial dilutions of single-stranded synthetic miR-122 (Dharmacon) as a standard.

miR-122 and HCV RNA quantitation in chimpanzee samples

Total RNA was extracted from serum and liver using RNA Bee (Leedo Medical Labs, Houston, TX), chloroform extraction and isopropanol precipitation. Detection of miR-122 was performed using primers and probes for miR-122 included in the ABI TaqMan assay (Cat No. 4373151) and the ABI TaqMan microRNA Reverse Transcription Kit (Cat No. 4366596). The RT reaction was performed with 5 ng of total cell RNA, and the PCR amplification was performed with one-tenth of the resulting cDNA. The RT reaction was performed at 16°C for 30 min, followed by 42°C for 30 min, and 85°C for 5 min. The TaqMan Universal PCR Master Mix with no AmpErase UNG was used for PCR amplification with reaction conditions of 95°C for 10 min followed by 40 cycles at 95°C for 15 sec and 60°C for 1 min. A standard curve was generated using a synthetic RNA equivalent to mature miR-122. HCV viral RNA levels in the serum and liver were determined using a real-time, quantitative RT-PCR (TaqMan) assay detecting sequences in the viral 5' noncoding RNA using an ABI 7500 sequence detector (PE Biosystems, Foster City, CA) as previously described [30]. Synthetic HCV RNA was used to generate a standard curve for determination of genome equivalents. The forward primer was from nucleotide 149 to 167 (5'-tgcggaaccggtgagtaca-3'), the reverse primer was from nucleotide 210 to 191 (5'-cgggtttatccaagaaagga-3') and the probe was from nucleotide 189 to 169 (5'-ccggtcgtcctggcaattccg-3') in the 5' NCR of HCV.

Affymetrix array analysis

Human RNA samples were subjected to high-density oligonucleotide microarray analysis as described previously [28]. In brief, cDNA amplified using the WT-Ovation Pico RNA Amplification System (NuGen, San Carlos, CA, USA) was used for fragmentation and biotin labeling with the FL-Ovation cDNA Biotin Module V2 (NuGen). Biotin-labeled cDNA suspended in hybridization cocktail (NuGen) was hybridized to Affymetrix U133 Plus 2.0 GeneChips, followed by labeling with streptavidin-phycoerythrin. Probe hybridization was determined using a GeneChip Scanner 3000 (Affymetrix) and analyzed using GeneChip Operating Software 1.4 (Affymetrix).

Statistical analysis

Statistical analyses were carried out using Prism V software (Graphpad Software, Inc). The paired t test was used for comparison of results arising from groups of paired tissue specimens (HCC versus non-tumor tissue), while the unpaired t test or Mann-Whitney test was used for comparisons between groups of unrelated tissues (e.g., HBV versus HCV infection). Nonparametric analysis of the correlation between miR-122 and ISG expression levels was done by the Spearman method. Other statistical tests were as described in the text.

Results

miR-122 abundance in HCV- versus HBV-associated liver cancer

We measured miR-122 abundance in paired tumor and non-tumor tissues collected from 26 patients undergoing surgical resection of HCC: 16 with concomitant chronic HCV infection, and 10 infected with HBV. The age, gender, histological classification of HCC, and fibrosis score of non-tumor tissues are shown in Figure 1 (see also Table 1). Subjects infected with HCV (predominantly genotype 1b) were approximately one decade older than those with HBV infection (66.6 ± 8.0 s.d. versus 54.3 ± 9.1 s.d. years, p=0.001, Figure 1A), consistent with previous studies indicating that HCC is generally diagnosed at an earlier age in HBV-infected Japanese patients [31]. There were no significant differences in the histological classification of HCC or scores for fibrosis or inflammatory activity in non-tumor tissues between the two groups (Figure 1B and C, and Table 1). There were more females among those with HCV infection (10 male and 6 female) than HBV (9 male and 1 female), but this difference did not achieve statistical significance (Chi square test with Yate's correction).

qRT-PCR revealed significant differences in the abundance of miR-122 in both tumor and non-tumor tissue samples when the HBV- and HCV-infected groups were compared (Figure 2). miR-122 abundance (miR-122 copy number per µg total RNA) was significantly lower in HCC tissue from HBV-infected versus HCV-infected subjects (p=0.009 by two-sided t test). In contrast, the miR-122 abundance in non-tumor tissue from HBV-infected patients was significantly greater than that in the HCV-infected patients (p=0.0005 by two-sided t test). The mean miR-122 abundance in HCC tissue was less than half that in non-tumor tissue in HBV-infected patients (p=0.003 by two-sided, paired t test). Strikingly, this relationship was reversed in the HCV-infected patients, in whom miR-122 abundance in HCC tissue was almost twice that in the non-tumor tissue (p=0.008 by two-sided paired t test). There was no significant difference in the abundance of miR-122 in the non-tumor tissue from HBV-infected patients and HCV-associated

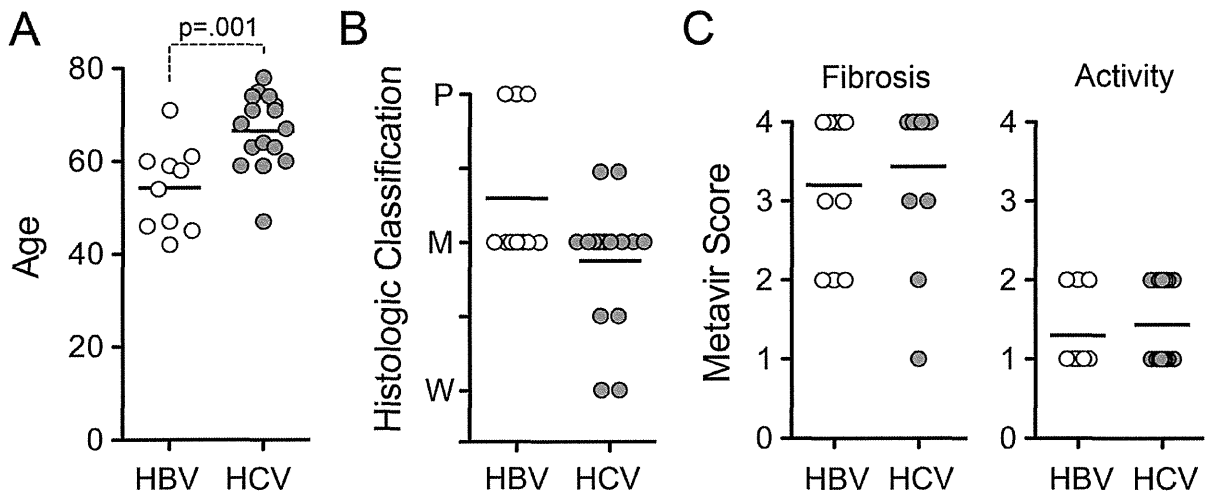

Figure 1. Age, histological classification of tumors, and scoring of non-tumor tissue for inflammation and fibrosis. (**A**) Age of subjects from whom HBV- and HCV-associated HCC and paired non-tumor samples were obtained. (**B**) Histological classification of tumors: W = well differentiated, M = moderately differentiated, P = poorly differentiated. (**C**) Individual scores for fibrosis and inflammatory activity in non-tumor tissue. Bars represent mean values. See also Table 1.

doi: 10.1371/journal.pone.0076867.g001

HCC. miR-122 abundance varied quite widely in liver tissue collected from non-infected individuals undergoing resection of metastatic tumors. Despite this, miR-122 abundance was significantly less in HBV-associated cancer tissue and non-tumor HCV-infected tissue than in the non-infected tissues (p=0.016 and 0.013, respectively).

To account for potential differences in degradation of the RNA or efficiency of reverse transcription between tissue samples, we assessed the abundance of several other small RNAs against which we could normalize the abundance of miR-122. U6, a noncoding snRNA component of the spliceosome, is commonly used to normalize miRNA abundance. However, we observed substantial differences in U6 abundance in these tissues, suggesting that U6 would be a poor normalizer (Figure 3A). Substantially less variation was observed in the abundance of the miRNAs, miR-24 or Let-7a (Figure 3B and C), for which the standard deviation of the critical threshold [25] in the PCR assay was 0.79 and 1.27, respectively, compared to 1.34 for U6. Notably, we observed no difference in the abundance of Let-7a in HBV-associated cancer and non-tumor tissues (p=0.52 by two-sided, paired t test), despite a prior report suggesting that Let-7a expression is regulated by the HBx protein and increased in abundance in HBV-associated HCC [32]. In addition, although miR-24 negatively regulates the expression of hepatocyte nuclear factor 4-alpha (HNF4-alpha) and thus might be up-regulated in some liver cancers [33], we did not observe this. A strong positive correlation was evident between the abundance of miR-24 and Let-7a (Figure 3E, Spearman r_s=0.7959, p<0.001 by two-tailed t test), suggesting that these miRNAs might belong to a common regulatory network and that either could be used to normalize miR-122 abundance. In contrast, there was no correlation between miR-24 and either U6 or miR-122 abundance (Figure 3D and F), which indicates that U6 and miR-122 are regulated independently of miR-24. Importantly, when the miR-122 abundance was normalized to miR-24 levels, miR-122 expression remained significantly depressed in HBV-associated HCC when compared either with paired non-tumor tissue, or HCC tissue from HCV-infected subjects (p<0.001 and p=0.002, respectively, Figure 2B). In replicate assays, the abundance of miR-122 in non-tumor HCV-infected tissue also remained significantly lower than either non-infected or HBV-infected liver tissues (Figure 2B). Similar associations were found when miR-122 abundance was normalized to Let-7a (data not shown).

To assess further the possibility of bias in these results due to differences in the quality of the RNA samples, we compared the RNA integrity number (RIN) [29] of each sample with the abundance of each of the small RNAs detected. Interestingly, while the quantity of U6 snRNA detected correlated positively with the RIN score (Spearman r_s = 0.5216, two-tailed p = 0.0001) (Figure S1A in Supporting Information), this was not the case with miR-24 or Let-7a (r_s = -0.124 and -0.045, respectively). RIN scores also did not vary significantly between tumor and non-tumor tissue-derived RNA samples, or RNA from HBV- vs. HCV-infected tissue. Thus, although the quality of the RNA samples was generally high (mean RIN = 8.0 ± 0.17 s.e.m.), it was an important factor in determining the abundance of U6 but not either of these miRNAs. These data suggest that U6 is less stable than the miRNAs and provide additional support for the use of miR-24 (or Let-7a) as a standard against which to normalize miR-122 abundance (see Discussion). Nonetheless, when miR-122 results were normalized to U6 abundance, the correlations described above

Table 1. Characteristics of Study Subjects.

	HCV (n = 16)	HBV (n=10)	Non-infected (n=9)
Mean Age (years)	66.6 ± 8.0 s.d.	54.3 ± 9.1	60.1 ± 14.3
Gender (M/F)	10M/6F	9M / 1F	5M / 4F
HCV Genotype			
1a	0	n/a	n/a
1b	14		
2	2		
3	0		
Fibrosis Stage	n (%)	n (%)	n (%)
0	0 (0)	0 (0)	9 (100)
1	1 (6)	0 (0)	0 (0)
2	1 (6)	3 (30)	0 (0)
3	4 (25)	2 (20)	0 (0)
4	10 (63)	5 (50)	0 (0)
Inflammation	n (%)	n (%)	n (%)
0	0 (0)	0 (0)	9 (100)
1	9 (56)	7 (70)	0 (0)
2	7 (44)	3 (30)	0 (0)
3	0 (0)	0 (0)	0 (0)
4	0 (0)	0 (0)	0 (0)
HCC Histologic Differentiation	n (%)	n (%)	
Well	2 (13)	0 (0)	n/a
Moderate-Well	2 (13)	0 (0)	
Moderate	10 (63)	7 (30)	
Poor-Moderate	2 (13)	0	
Poor	0 (0)	3 (30)	
IL28B genotype (rs8099917)	n (%)		
TT	9 (56)	n.d.	n.d.
TG	7 (44)		
GG	0 (0)		

n/a = "not applicable"; n.d. = "not done"

doi: 10.1371/journal.pone.0076867.t001

between miR-122 abundance, in both tumor and non-tumor tissues, and the type of virus infection remained strongly statistically significant (Figure S1B in Supporting Information). The mean miR-122 abundance was substantially lower in HBV-associated HCC tissue than in HBV-infected non-tumor tissue ($p = 0.003$ by paired t-test), while this relationship was reversed in HCV-infected liver ($p = 0.001$). miR-122 abundance was also significantly lower in non-tumor tissue from HCV-infected subjects than HBV-infected subjects ($p < 0.001$).

To exclude the possibility of bias due to the trend toward a less differentiated histologic classification among HBV-associated cancers (Figure 1B), we limited the comparison of miR-122 abundance to those HCC tissues that were scored as moderately differentiated and their corresponding paired non-tumor samples. While this reduced the number of subjects available for analysis, miR-122 abundance remained significantly lower in HBV- versus HCV-associated cancer tissue: $p=0.007$ when compared on the basis of miR-122 copy number/mg RNA (Figure 2C) vs. $p=0.033$ when normalized to miR-24 (Figure 2D). Thus differences in miR-122 abundance in HCC associated with HBV vs. HCV infection are independent of the degree of histologic differentiation of the cancer.

Collectively, these results provide strong evidence that miR-122 expression is reduced in HCC associated with HBV infection, but not in most HCV-associated liver cancers.

Reduced miR-122 abundance is associated with interferon responses in HCV-infected liver

The data shown in Figure 2 indicate that miR-122 is frequently reduced in abundance in non-tumor, HCV-infected liver tissue, but not in liver infected with HBV. To determine whether similar HCV-induced suppression of miR-122 expression occurs in chimpanzees (*Pan troglodytes*), the only animal species other than humans that is permissive for HCV infection, we measured miR-122 abundance in liver tissues

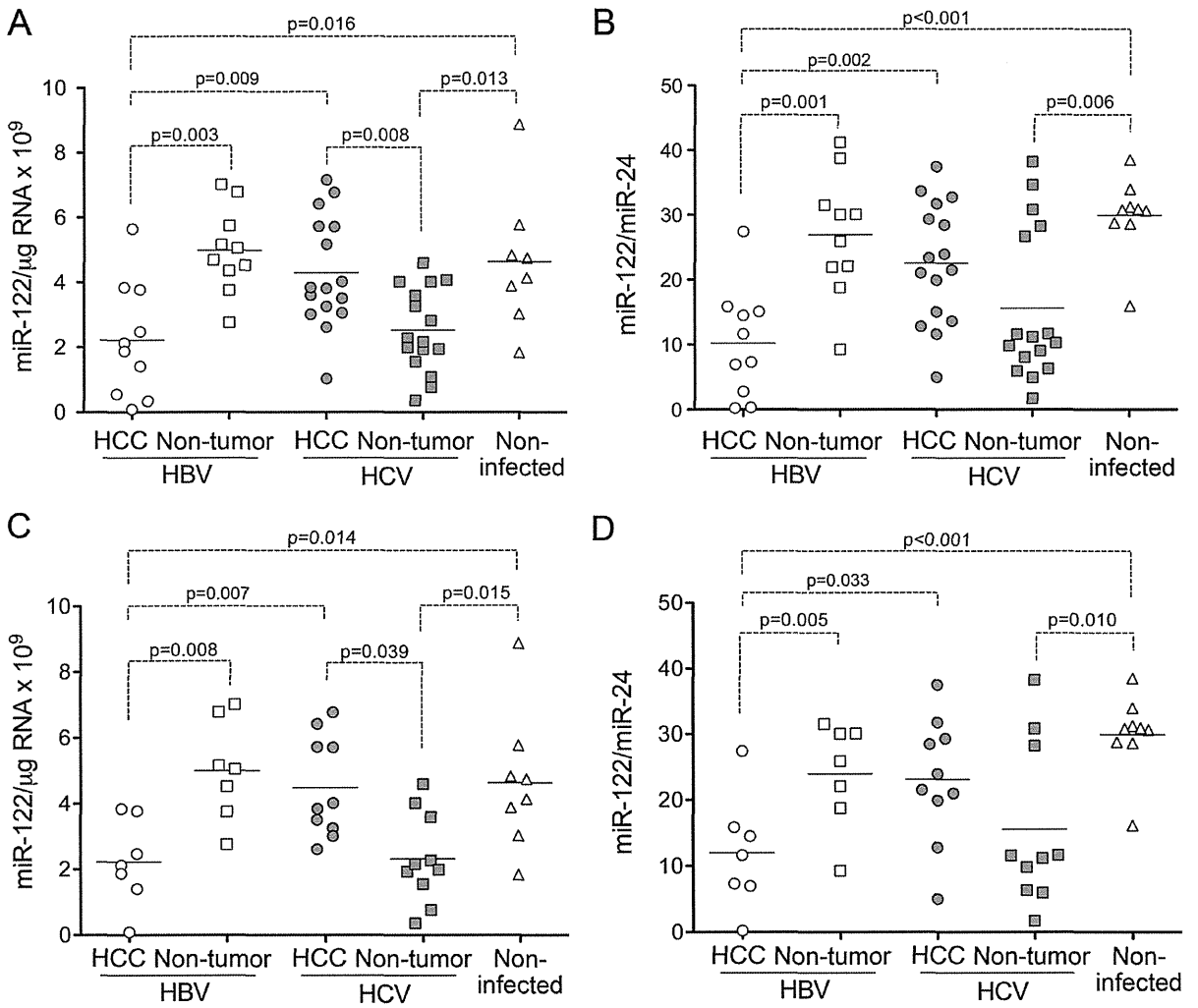

Figure 2. miR-122 expression in paired HCC and non-tumor liver tissue from patients with chronic HBV and HCV infection and control, non-infected liver tissue. (**A**) miR-122 abundance quantified by qRT-PCR in paired tumor and non-tumor tissues and non-infected ('normal') liver from patients undergoing resection of metastatic tumors, normalized to total RNA. (**B**) Relative miR-122 abundance normalized to miR-24 abundance in the same tissues. (**C**) miR-122 abundance in HCC classified histologically as "moderately differentiated", paired non-tumor tissue from the same patients, and non-infected ('normal') liver. (**D**) miR-122 abundance in the subset of tissues shown in panel C, normalized to miR-24 abundance. The statistical significance of differences between paired observations was estimated using the paired t test, while differences between non-paired observations were analyzed by the Mann-Whitney test.

doi: 10.1371/journal.pone.0076867.g002

collected previously from 45 HCV-infected chimpanzees, and compared this to that present in 10 HBV-infected animals, and 6 that were not infected with either virus. These results showed that miR-122 expression was significantly reduced in HCV-infected liver compared to both HBV-infected ($p<0.0001$) and normal, non-infected ($p=0.007$) chimpanzee liver (Figure 4A). A strong, negative correlation (Spearman $r_s= -0.63$, $p<0.0001$) existed between hepatic miR-122 expression levels and HCV RNA copy numbers in serum (Figure 4B). The mean miR-122 abundance was lower in HBV-infected liver than in uninfected chimpanzee liver (Figure 4A), but the difference did not achieve statistical significance ($p=0.059$ by two-tailed t test). Thus, intra-hepatic miR-122 abundance is reduced in HCV-infected chimpanzees as well as humans. This is consistent with earlier studies that have found reduced intrahepatic expression of miR-122 in patients with advanced chronic hepatitis C [34–36].

Sarasin-Filipowicz et al. [36] reported previously that miR-122 levels were reduced in liver from HCV-infected

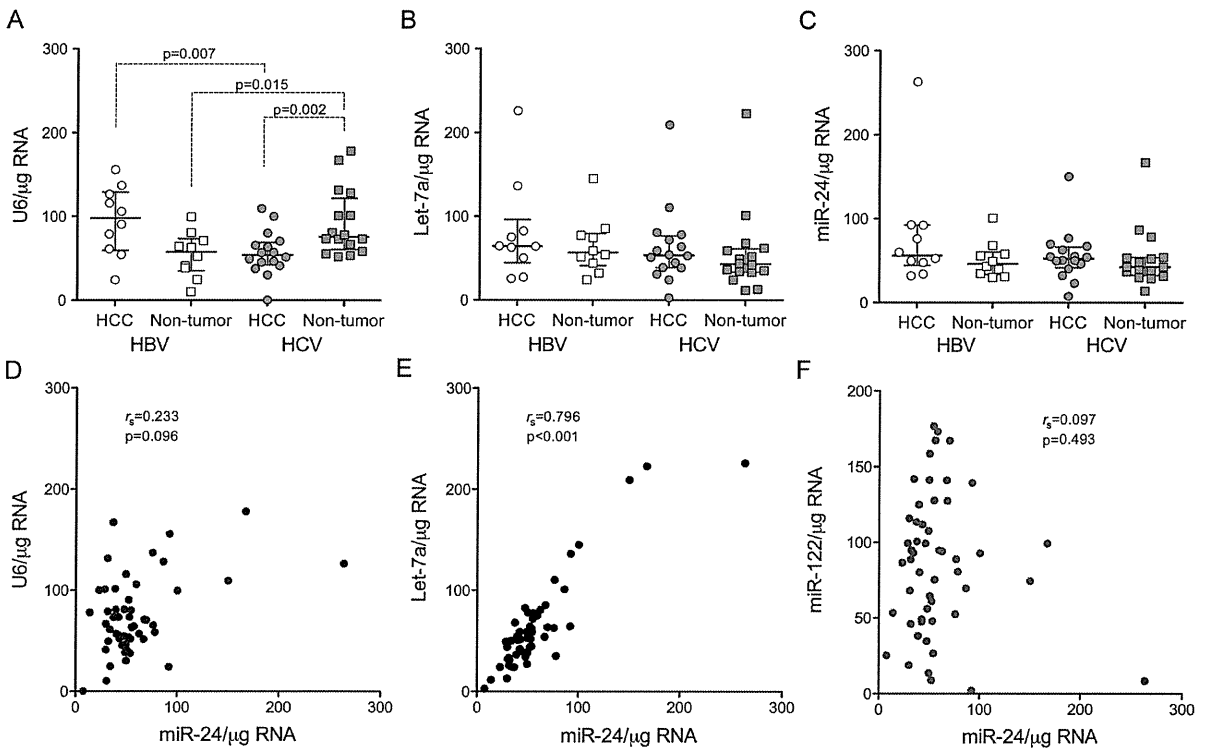

Figure 3. Comparison of small RNAs as normalizers for assessing miR-122 abundance. Shown in the panels at the top are the relative abundance of (**A**) U6 snRNA, (**B**) Let-7a, and (**C**) miR-24 miRNAs in paired tumor and non-tumor tissues from subjects with HBV or HCV infection, normalized to total RNA. Bars represent median and quartiles for each group. Statistical comparisons between groups were made with paired or unpaired t tests, and are shown only if p<.05. In the lower set of panels, (**D**) U6, (**E**) Let-7a, and (**F**) miR-122 abundance are plotted as a function of miR-24 abundance. r_s = Spearman rank-order correlation coefficient.

doi: 10.1371/journal.pone.0076867.g003

patients who responded poorly to treatment with pegylated IFN-α and ribavirin (Peg-IFN/RBV). Consistent with this, we observed a negative correlation between miR-122 abundance in non-tumor tissue from HCV-infected human subjects and the GT versus TT genotype at the rs8099917 locus in the IL28B gene (p=0.011, Figure 5A) that is predictive of a poor response to Peg-IFN/RBV therapy [37]. HCV-infected patients with the TT genotype are prone to a greater inflammatory response than those with TG or GG [38]. Thus, differences in IL28B genotype may have contributed to a correlation we observed between miR-122 abundance and A1 versus A2 Metavir activity scores (Figure 5B, 6 of 7 subjects with an A2 Metavir score had the TT genotype). Importantly, the association between IL28B genotype and miR-122 abundance was observed only in non-tumor liver from HCV-infected patients, and not in paired HCC tissue (Figure 5A).

Patients who are non-responsive to Peg-IFN/RBV, or who have IL28B genotypes predictive of a poor response to Peg-IFN/RBV therapy, are likely to have increased pre-treatment intra-hepatic ISG transcript levels compared to those who respond well to treatment [39–41]. We thus asked whether a correlation existed between miR-122 abundance and levels of selected ISG transcripts in HCV-infected non-tumor tissue determined by Affymetrix 133U Plus 2.0 GeneChip assay. For this analysis, we selected ISGs that were shown previously to be correlated with treatment response [39] (Figure 5C). We also included Mx1 and OAS1, both well-characterized ISGs. Overall, the Affymetrix signals for these genes showed a strong trend toward negative correlations with miR-122 abundance. Fourteen of 24 ISGs demonstrated a Spearman rank-order coefficient, $r_s \leq -0.300$; this negative correlation was significant ($p<0.05$) for 7 of the ISGs by one-tailed t test (Figure 3C). These data are consistent with the notion that reduced miR-122 abundance is associated with strong intrahepatic IFN-mediated responses to the virus.

miR-191 abundance is increased in HBV-associated HCC

Since Elyakim et al. [42] reported recently that miR-191 was increased in HCC arising in a study population comprised mostly of HBV-infected subjects, we also quantified miR-191 expression levels in the human tissue samples. We confirmed

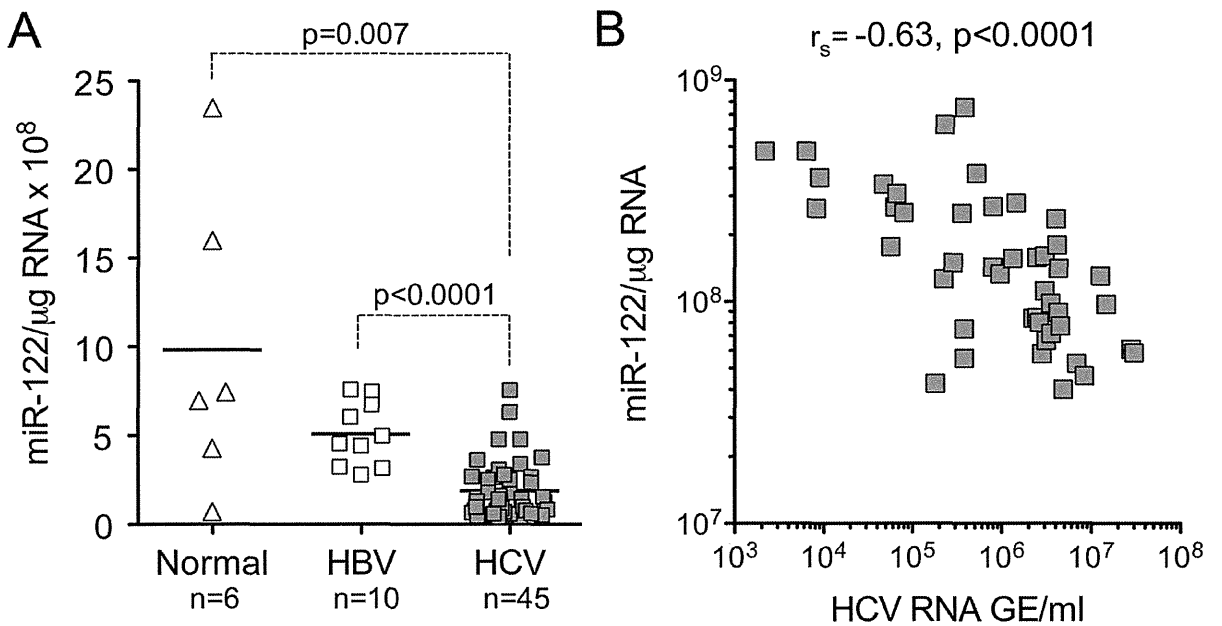

Figure 4. miR-122 expression in chimpanzee liver tissue. (**A**) Hepatic miR-122 abundance in liver biopsies from chimpanzees infected with HBV or HCV, or not infected with either virus ('normal'). Statistical significance was assessed by non-paired two-sided t test. Bars represent mean values. (**B**) Liver miR-122 expression plotted against serum HCV RNA abundance from acutely HCV-infected chimpanzees. r_s = Spearman rank-order correlation coefficient.

doi: 10.1371/journal.pone.0076867.g004

miR-191 levels were modestly increased in HBV-associated HCC compared to non-tumor HBV-infected tissue when normalized to total RNA (p=0.049 by two-sided, paired t test, Figure 6). This trend remained significant only by one-sided t test when the miR-191 abundance was normalized to miR-24 abundance (p=0.045), and was absent when miR-191 levels were normalized to U6 snRNA. miR-191 abundance in non-tumor, HBV-infected tissue was similar to that in both tumor and non-tumor liver from HCV-infected subjects (Figure 6).

Discussion/Conclusions

miR-122 is a critical regulator of hepatic gene expression and an essential host factor for HCV replication [15,18,43]. It also has important tumor suppressor properties [16,44], and recent reports indicate that loss of its expression promotes carcinogenesis in knockout mice [45,46]. While its abundance is often reduced in HCC [21,22], two previous studies suggest that miR-122 expression may be preserved in liver cancer arising in patients with HCV infection [24,25]. We confirm this, showing in a genetically and geographically homogeneous population of patients, and normalizing results either to total RNA or to levels of miR-24, that miR-122 abundance is significantly reduced from normal in HBV-associated HCC but not in liver cancer associated with HCV infection (Figure 2A and B). This difference in miR-122 expression is independent of the histologic classification of the tumors (Figure 2C and D), as well as the degree of fibrosis or inflammation in paired non-tumor tissue from the same patients. Conversely, we show that miR-191 tends to be increased in abundance in HBV-associated cancer, but not HCV-associated HCC (Figure 6). These observations have important implications for the pathogenetic mechanisms involved in viral carcinogenesis within the liver. While HCC may arise as a result of factors common to both HBV and HCV infection (such as chronic inflammation, oxidative stress, and progressive fibrosis leading to cirrhosis), distinctive molecular signatures associated with HBV- versus HCV-associated cancer suggest there are fundamental differences in the ways these two viruses cause cancer.

Our study highlights the challenges inherent in comparing miRNA abundance in different clinical samples. In addition to potential differences in the proportion of cells present within a biopsy that are of hepatocellular origin vs. derived from other cell lineages, a constant concern is the quality of the RNA. While our initial analysis, like many studies, compared miR-122 copy numbers based on the quantity of total RNA subjected to RT-PCR, this approach can be biased by differences in the quality of the RNA and degree of RNA degradation. Although our RNA samples were of generally high quality (see Figure S1A in Supporting Information), we determined miR-24, Let-7a, and U6 snRNA copy numbers and evaluated each as a standard against which miR-122 abundance could be normalized to account for potential differences in RNA integrity (Figure 3). Median miR-24 and Let-7a copy numbers did not

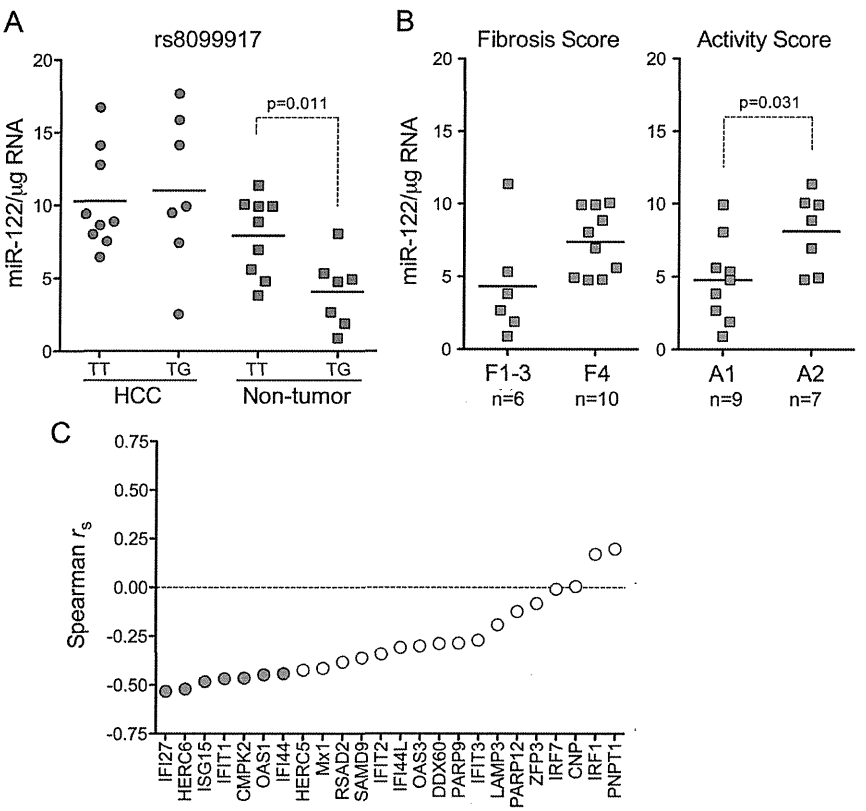

Figure 5. miR-122 expression, IL28B genotype, Metavir scores and ISG transcript levels in HCV-infected human liver. (**A**) miR-122 expression in HCC and paired non-tumor samples from subjects with HCV infection, grouped according to rs8099917 genotype (TT or GT). (**B**) miR-122 expression levels in non-tumor tissue from HCV-infected subjects categorized according to Metavir score for (left) fibrosis and (right) inflammatory activity. (**C**) Correlation between miR-122 abundance and expression levels of selected ISGs determined by Affymetrix U133 Plus 2.0 Array analysis. With the exception of OAS1 and Mx1, intrahepatic transcript levels of these ISGs have been shown previously to be predictive of Peg-IFN/RBV treatment outcome [31]. "r_s" = Spearman rank-order correlation coefficient. Filled symbols indicate a statistically significant negative correlation ($p<0.05$ by one-sided t test).

doi: 10.1371/journal.pone.0076867.g005

vary significantly between tumor and non-tumor tissue samples from HBV- and HCV-infected subjects (one-way ANOVA), suggesting that the expression of these miRNAs is relatively constant in liver and that either could serve as a standard for normalizing miR-122 abundance. In contrast, median U6 copy numbers varied significantly between these tissue groups ($p = 0.004$ by one-way ANOVA with Kruskal-Wallis test) and, more importantly, were strongly correlated negatively with the RIN score, a measure of RNA integrity [29] (Figure S1A in Supporting Information). There was no correlation between the RIN score and miR-24 or Let-7a abundance, suggesting that U6 snRNA may be less stable and more prone to degradation than the miRNAs. This may be due to the greater length of U6 (106 nts vs. ~20-23 nts for miRNAs), or the absence of terminal modifications that may influence the stability of miRNAs [47]. Consistent with this, Let-7a was found to have greater biological stability and to be superior to U6 for normalization of miRNA abundance in previous studies of rat hepatocyte RNA [48]. Nonetheless, even though these data argue against the use of U6 as a standard for normalizing miR-122 copy numbers, we found the abundance of miR-122 was significantly reduced in HCC associated with HBV but not HCV infection, and that miR-122 abundance was significantly depressed in non-tumor tissue infected with HCV but not HBV, using any of these small RNAs, including U6, to normalize the miR-122 results.

While it remains unclear exactly how miR-122 contributes to the HCV lifecycle, it is known to promote viral replication independently of its regulation of hepatic genes [49]. It binds to two sites near the 5' end of the viral genome [18], recruiting argonaute 2 (EIF2C2) and physically stabilizing the RNA by protecting it from 5' exonucleolytic Xrn1-mediated decay [19,20]. However, miR-122 has other, positive effects on HCV replication beyond its ability to physically stabilize the viral

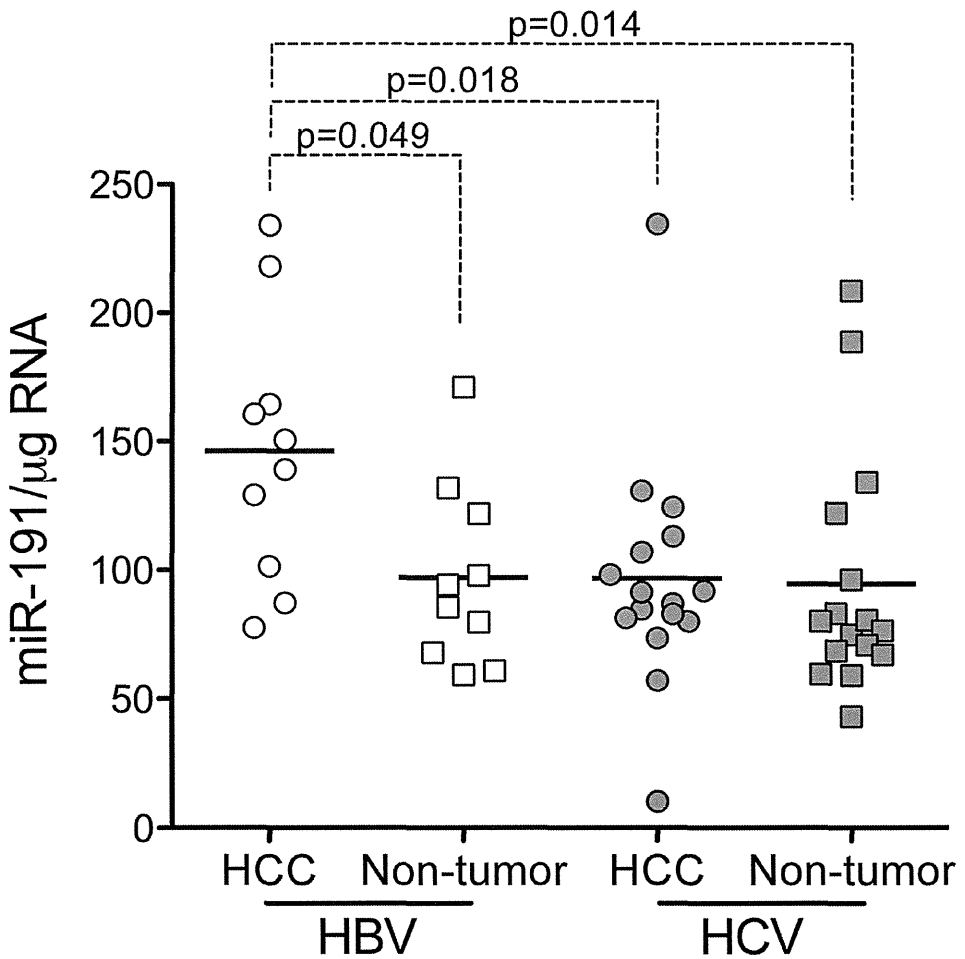

Figure 6. Relative abundance of miR-191 in paired HCC and non-tumor tissue from subjects with HBV or HCV infection. Relative miR-191 abundance in paired tumor and non-tumor samples from HBV- and HCV-infected subjects normalized to total RNA. Statistical significance was assessed in two-sided paired t tests for comparisons between tumor and non-tumor tissue, or two-sided unpaired t test for comparison between infection groups.

doi: 10.1371/journal.pone.0076867.g006

genome [20,50]. It is essential for HCV replication, and its therapeutic silencing with an antisense oligonucleotide has potent antiviral effects [15,51]. No other RNA virus is known to rely so completely on a cellular miRNA for its replication cycle. Thus, the continued expression of miR-122 in HCV-associated HCC could reflect close linkage between carcinogenesis and HCV replication and viral protein expression. We speculate that miR-122 expression is preserved in HCV-associated HCC (in contrast to HBV-associated cancer) because HCV-encoded proteins help to drive a multi-stage process of carcinogenesis within infected cells. This may result from the ability of the virus to directly disable DNA damage responses or other cellular tumor suppressor functions, and to contribute directly to malignant conversion of hepatocytes as reviewed elsewhere [10,52]. Early loss of miR-122 during the progression to cancer would eliminate virus replication, protecting the cell from further effects of viral protein expression. In contrast, in HBV-infected cells, a loss of miR-122 expression could both accelerate tumorigenesis and enhance replication, as miR-122 appears to restrict, rather than promote, HBV replication [53–56]. Although speculative, this hypothesis raises the interesting possibility that HCV-associated cancers arise within the small minority of hepatocytes infected with the virus, and not the much larger number of uninfected bystander cells [52,57].

Epigenetic mechanisms are likely to contribute to the differential expression of miR-122 and miR-191 in HCC. The miR-122 promoter is hyper-methylated in the HBV-associated HCC-derived cell line, Hep3B [58]. It remains to be seen whether differences exist in methylation of the promoter in vivo in HBV- versus HCV-associated cancers, but bacterial artificial